

8-2011

DEVELOPMENTAL DEREGLATION AND TUMORIGENESIS INHIBITION IN 14-3-3ZETA KNOCKOUT MOUSE

Jun Yang

Follow this and additional works at: https://digitalcommons.library.tmc.edu/utgsbs_dissertations



Part of the [Cancer Biology Commons](#), [Developmental Biology Commons](#), and the [Molecular Biology Commons](#)

Recommended Citation

Yang, Jun, "DEVELOPMENTAL DEREGLATION AND TUMORIGENESIS INHIBITION IN 14-3-3ZETA KNOCKOUT MOUSE" (2011). *The University of Texas MD Anderson Cancer Center UTHealth Graduate School of Biomedical Sciences Dissertations and Theses (Open Access)*. 175.
https://digitalcommons.library.tmc.edu/utgsbs_dissertations/175

This Dissertation (PhD) is brought to you for free and open access by the The University of Texas MD Anderson Cancer Center UTHealth Graduate School of Biomedical Sciences at DigitalCommons@TMC. It has been accepted for inclusion in The University of Texas MD Anderson Cancer Center UTHealth Graduate School of Biomedical Sciences Dissertations and Theses (Open Access) by an authorized administrator of DigitalCommons@TMC. For more information, please contact digitalcommons@library.tmc.edu.

**DEVELOPMENTAL DEREGULATION AND TUMORIGENESIS INHIBITION IN
14-3-3ZETA KNOCKOUT MOUSE**

by

Jun Yang, B.Sc.

APPROVED:

Dihua Yu, M.D., Ph.D.
Supervisory Professor

Michael Andreeff, M.D., Ph.D.

Richard Behringer, Ph.D.

Mien-Chie Hung, Ph.D.

Wei Zhang, Ph.D.

Bin Wang, Ph.D.

APPROVED:

Dean, The University of Texas
Graduate School of Biomedical Sciences at Houston

**DEVELOPMENTAL DEREGULATION AND TUMORIGENESIS INHIBITION IN
14-3-3ZETA KNOCKOUT MOUSE**

A DISSERTATION

Presented to the Faculty of

The University of Texas

Health Science Center at Houston

and

The University of Texas

M. D. Anderson Cancer Center

Graduate School of Biomedical Sciences

in Partial Fulfillment

of the Requirements

for the Degree of

DOCTOR OF PHILOSOPHY

by

Jun Yang, B.Sc.

Houston, Texas

August, 2011

Copyright

Figure 1 and 3 were adapted from Polyak et al, *Biochimica et biophysica acta*, 2001 and Rittinger et al, *Mol Cell*, 1999 with written permission from the publisher.

DEDICATION

This dissertation is dedicated to those who suffered from cancer. Their experience of fighting cancer motivated me to study the disease. I truly hope this research can benefit some of them sometime in the future. I also dedicate this thesis to my previous mentor, Dr. Li Jin and Dr. Yonglian Zhang. They helped me build up basic research attitude and skills to search for the truth. To my respected scientist Dr. Zaiping Li who encouraged me to do top notch science to benefit the society. To my friends who supported me all these years. I appreciate them. Most importantly I dedicate this dissertation to my family especially my wife Tingfang and my son Kevin. I would not be able to accomplish this without them. Their support helped me keep moving on when I was down and finally can be here writing this down.

ACKNOWLEDGEMENT

First of all, I MUST thank my mentor, Dr. Dihua Yu for giving me this interesting project. I thank her for the support and patience along all these years. Her dedication to cancer research is always a role model for me to learn from. I thank all lab members in Dr. Yu's lab, present and previous ones especially Qingfei Wang, Yan Xiong, Hai Wang and Ping Li for their tremendous help, invaluable suggestions. I thank my committee members, Drs. Richard Behringer, Sharon Dent, Randy Johnson, Miles Wilkinson, Xin Lin, Elsa Flores, Angabin Matin, Wei Zhang, Michael Andreeff and Mien-Chie Hung. Their criticism and suggestions helped me carry the project forward. I also thank the Cancer Biology Program at GSBS. This excellent program provided a great environment for scientific interaction among students and faculties. Their input helped me think about my project from different angles thus making the project get more comprehensive and into depth. Finally I thank all those who cared and supported this research project including the tax payers, grants funding and donations.

DEVELOPMENTAL DEREGLATION AND TUMORIGENESIS INHIBITION IN 14-3-3ZETA KNOCKOUT MOUSE

Publication No. _____*

Jun Yang, B.Sc.

Supervisory Professor: Dihua Yu, M.D., Ph.D.

Cancer is second leading cause of death in the United States. Improving cancer care through patient care, research, education and prevention not only saves lives, but reduces health care cost as well. Breast cancer is the most leading cause of cancer incidence and cancer related death in women of the United States. 14-3-3s are a family of conserved proteins ubiquitously expressed in all eukaryotic organisms. They form complexes with hundreds of proteins by binding to specific phospho-serine/threonine containing motifs. In this way they regulate a variety of cellular processes and are involved in many human diseases especially cancer to our interest. Our lab and others recently reported that the 14-3-3 ζ (zeta) isoform is overexpressed in ~45% breast cancers, which predicted poor patient outcome. 14-3-3 ζ overexpression confers chemotherapy resistance. Additionally, 14-3-3 ζ prevents anoikis by suppressing p53 and promotes epithelial mesenchymal transition by activating the TGF- β signaling pathway, which plays important roles during tumor formation and progression. Based on these I hypothesized that 14-3-3 ζ plays an important role in breast cancer.

To systematically study the role of 14-3-3 ζ in breast cancer *in vivo*, I generated a strong 14-3-3 ζ hypomorphic mutant mouse model by Gene Trap. We found that the homozygous mutant mice are lethal neonatally due to respiratory failure. This lethality could be rescued when outbred to CD-1 or backcrossed to FVB/N mouse strain.

Early mammary gland development was not significantly affected in 14-3-3 ζ homozygous mutant mice. When crossed with MMTV driven Polyoma Middle-T or Neu oncogene transgenic tumor prone mouse, the 14-3-3 ζ mutant mice had longer tumor latency and reduced lung metastasis compared to their wild type counterpart. The tumor samples from the 14-3-3 ζ mutant mice displayed reduced proliferation, increased apoptosis and reduced angiogenesis. Multiple genes were differentially expressed in the 14-3-3 ζ knockout tumors. MiR-126 was an important microRNA mediating both the lethality and tumorigenesis inhibition phenotype.

In addition, 14-3-3 ζ knockout mice are smaller than their litter mates. This growth retardation was accompanied with reduced growth hormone but increased IGF-1 level in the circulation. The knockout mice had a defect in glucose homeostasis. They have lower blood glucose and tolerate glucose better than their wild type counterparts due to reduced glucose uptake. The aberrant glucose homeostasis was accompanied by reduced Hif1- α and Igf1r expression.

The 14-3-3 ζ knockout mice had other phenotypes that need to be further characterized. This mouse strain provided new resource to study 14-3-3 ζ function *in vivo* and potentially could benefit patients that have aberrant expression of 14-3-3 ζ .

TABLE OF CONTENT

Copyright	pg. iii
Dedication	pg. iv
Acknowledgement	pg. v
Abstract	pg. vi
Table of content	pg. ix
List of figures	pg. xi
List of tables	pg. xiv
Abbreviation	pg. xv
Chapter 1 – Introduction	pg. 1
1.1 Cancer	pg. 1
1.2 Breast cancer	pg. 3
1.3 14-3-3 family proteins	pg. 6
1.4 14-3-3 ζ	pg. 13
1.5 microRNA-126	pg. 15
Purpose, Rationale and Significance	pg. 17

Chapter 2 - Material and Methods	pg. 18
Chapter 3 – Results and Discussion	pg. 25
3.1 Generation of 14-3-3 ζ knockout mouse	pg. 25
3.2 14-3-3 ζ knockout mice are lethal neonatally	pg. 35
3.3 Loss of 14-3-3 ζ inhibited mammary gland tumorigenesis and lung metastasis	pg. 47
3.4 14-3-3 ζ knockout mice are growth retarded	pg. 70
3.5 Other phenotypes in 14-3-3 ζ knockout mouse	pg. 85
Chapter 4 – Summary and Future Direction	pg. 87
Reference	pg. 89
Vita	pg. 111

LIST OF FIGURES

Figure 1. Schematic of breast cancer tumorigenesis and progression	pg. 5
Figure 2. 14-3-3 ζ crystal structure	pg. 9
Figure 3. 14-3-3s share high similarity in amino acid sequence and crystal structure	pg. 10
Figure 4. RT-PCR confirmation that the ES cell line RRR334 had 14-3-3 ζ inactivated	pg. 27
Figure 5. Determination of gene trap vector integration site in 14-3-3 ζ genome using PCR	pg. 28
Figure 6. Genotyping of 14-3-3 ζ mutant mouse	pg. 29
Figure 7. 14-3-3 ζ is significantly downregulated in homozygous mutant mouse mammary gland	pg. 31
Figure 8 14-3-3 ζ N-terminal fragment is non-functional	pg. 32
Figure 9. 14-3-3 ζ knockout mice had defect in lung development	pg. 39
Figure 10. 14-3-3 ζ did not affect proliferation and pneumocytes differentiation	pg. 40
Figure 11. Loss of 14-3-3 ζ lead to angiogenesis defect in lungs	pg. 41

Figure 12. MicroRNA-126 was downregulated in 14-3-3 ζ knockout lungs, pg. 43

Figure 13. Loss of 14-3-3 ζ did not significantly affect mammary gland
development pg. 49

Figure 14. Loss of 14-3-3 ζ inhibited tumorigenesis and lung metastasis pg. 51

Figure 15. 14-3-3 ζ expression is downregulated in the tumors from homozygous
mutant mice pg. 53

Figure 16. Loss of 14-3-3 ζ affected multiple aspects of cancer biology pg. 56

Figure 17. Loss of 14-3-3 ζ affected multiple signaling molecules expression
pg. 57

Figure 18. Loss of 14-3-3 ζ prolonged tumor latency induced neu oncogene
pg. 60

Figure 19. Neu oncogene expression was not affected in 14-3-3 ζ knockout
tumors pg. 61

Figure 20. Loss of 14-3-3 ζ affects tumor biology in Neu oncogene induced
tumors pg. 62

Figure 21. MicroRNA-126 was downregulated in 14-3-3 ζ knockout tumors
pg. 64

Figure 22. MicroRNA-126 regulates angiogenesis downstream of 14-3-3 ζ	pg. 66
Figure 23. 14-3-3 ζ knockout mice are growth retarded	pg. 71
Figure 24. Loss of 14-3-3 ζ lead to aberrance in growth related hormonal expression	pg. 74
Figure 25. Loss of resulted in lower blood glucose	pg. 77
Figure 26. 14-3-3 ζ regulates glucose uptake	pg. 78
Figure 27. 14-3-3 ζ regulates HIF1- α and IGF1R	pg. 81
Figure 28. 14-3-3 ζ knockout mice display phenotype indicative of neuronal degeneration	pg, 86

LIST OF TABLES

Table 1. 14-3-3z knockout mouse are lethal neonatally in C57Bl/6 genetic background and are viable in CD-1 background pg. 37

ABBREVIATIONS

2-NBDG, 2-(N-(7-nitrobenz-2-oxa-1,3-diazol-4-yl)amino)-2-deoxyglucose

ADH, atypical ductal hyperplasia

Akt, V-Akt murine thymoma viral oncogene

APC, APC gene, tumor suppressor lost in Adenomatous Polyposis of the Colon

AQP5, aquaporin protein 5

Bad, Bcl2 antagonist of cell death

Bax, Bcl2 associated x protein

BCR, breakpoint cluster region kinase

BRCA1//2, Breast cancer 1 and 2 gene

CD34, Hematopoietic progenitor cell antigen

Cdc25, cell division cycle 25

CJD, Creutzfeldt-Jakob Disease

DCIS, ductal carcinoma in situ

DMEM, Dulbecco's Modified Eagle Medium

E2F, E2F transcription factor

ELISA, Enzyme-linked immunosorbent assay

ErbB2, V-Erb-B2 Avian Erythroblastic leukemia viral oncogene homolog 2

Erk, extracellular-signal regulated kinase

FBS, fetal bovine serum

GEM, genetic engineered mouse

HA, Hemagglutinin tag

HIF1- α , hypoxia induced factor 1, alpha subunit

IACUC, Institutional Animal Care and Use Committee

IGF-1, insulin-like growth factor 1

IGF1R, insulin-like growth factor 1 receptor

IHC, immunohistochemistry

i.p., Intraperitoneal injection

IRS, immunoreactive score

IRS-1, insulin receptor substrate 1

i.v., intravenous injection

Ki67, Mki67 gene

MDS, Miller-Dieker Syndrome

Mek1, Mitogen activated protein kinase kinase

MMTV-LTR, Mouse mammary tumor virus, long terminal repeats

NES, nuclear exportation signal

Neu, oncogene derived from rodent glioblastoma cell line, ErbB2 homolog

Par3, partitioning defective protein 3

PDGF, platelet derived growth factor

PECAM1, CD31, platelet endothelial cell adhesion molecule 1

PKC, protein kinase C

PML, progressive multifocal leukoencephalopathy

PTEN, phosphatase and tensin homolog

PyMT, Polyoma middle T viral antigen

qRT-PCR, quantitative real-time reverse-transcription polymerase-chain-reaction

Raf-1, V-Raf-1 murine leukemia viral oncogene homolog 1

RIA, radio-immuno-assay

RISC, RNA-induced silencing complex

SP-A, surfactant pulmonary-associated protein A1

TGF- β , transforming growth factor beta

TGF β RI, Transforming growth factor beta receptor 1

TUNEL, Terminal deoxynucleotidyl transferase dUTP nick end labeling

VEGF, vascular endothelial growth factor

Chapter 1

Introduction

1.1 Cancer

1.1a Definition

Cancer, also termed as malignant neoplasm, is defined as a group of more than 100 diseases in which cells in a part of the body display uncontrolled growth, invade and destroy adjacent tissues, and very often spread to other locations of the body through lymphatic system or blood stream known as metastasis. It is different from benign tumor in which the cells do not proliferate without control, invade locally or metastasize to distant organs. Cancer, if left untreated, can cause serious illness and even death.

1.1b Cause

Cancer can be an inheritable genetic disease, like BRCA1/2 gene mutation in breast cancer, APC gene deletion in colon cancer and PTEN loss in many types of cancers. However, the majority of cancers are caused by environmental factors like exposure to alcohol, smoking, radiation, infection, diet and exercise etc. The most significant risk factor is aging.

1.1c Statistics

Cancer is the second leading cause of death in the states. More than 11 million people are suffering from cancer nowadays according to National Cancer Institute's Surveillance Epidemiology and End Results (SEER) database. It is estimated that about 40% people will develop cancer in their lifetime and more than 20% will die from it. The cost of cancer is more than 228 billion dollars annually. Improving cancer care through patient care, research, prevention and education is critical not only for eliminating cancer mediated suffering and death, but also for helping to keep the nation in good financial figure.

1.2 Breast cancer

1.2a Definition

According to the definition of National Cancer Institute, breast cancer is the type of neoplasm that forms in tissues of the breast, usually the ducts (tubes that carry milk to the nipple) and lobules (glands that make milk). It occurs in both men and women, although male breast cancer is rare. Like most cancers, breast cancer is influenced by many risk factors, like heritable genetic mutations, exposure to toxic chemicals, diet and living styles etc.

1.2b Statistics

Breast cancer is the most leading cause of cancer incidence and cancer related death in women of the United States. It is estimated that 230,480 women will develop breast cancer this year, and 39,520 will die from it. About one out of eight women will develop breast cancer in their life time. Thanks to the recent breast cancer care improvement, breast cancer is highly treatable if detected early with combination of surgery, chemotherapy, radiation therapy and hormone therapy. The five-year survival rate of breast cancer, when diagnosed at localized primary site, is over 98%. However, this rate drops to 23.4% if diagnosed as metastatic disease (data obtained from American Society of Cancer online).

1.2c Research models

Breast cancer development has been modeled as a multi-step process starting from normal mammary epithelium to ductal hyperplasia, atypical ductal hyperplasia (ADH), ductal carcinoma in situ (DCIS), invasive carcinoma, ending with tumors capable of metastasizing to distant organs. These steps are defined by a series of morphological changes based on epidemiological and histological observations (Figure 1) (1, 2). This model has been widely used to understand how breast cancer initiates and progresses into a killing disease.

However, breast cancer is not a single disease but a collection of heterogeneous diseases that have distinct histopathological features, genetic variability and diverse prognostic outcomes. It is realized that no individual model can completely recapitulate this complex disease (3).

Currently breast cancer cell lines, xenografts and genetically engineered mouse models are widely used in the field of breast cancer research to understand breast cancer from different angles (3).

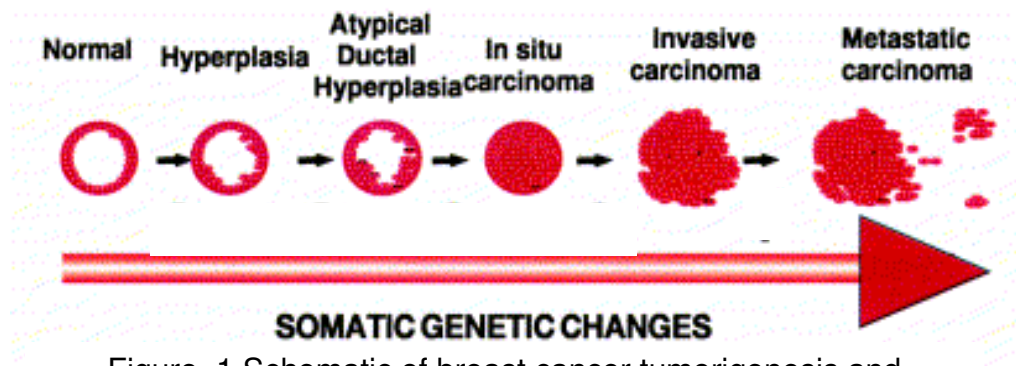


Figure. 1 Schematic of breast cancer tumorigenesis and progression

Polyak K. et. al. 2001

1.3 14-3-3 family proteins

1.3a General property

14-3-3s are a 28-33kd conserved family proteins ubiquitously expressed in all eukaryotic organisms (4). They were first found in 1967 as abundant proteins in bovine brain. The name of 14-3-3 was determined by their fraction number on a 2D DEAE-cellulose chromatography and the migration position in subsequent starch gel electrophoresis (5). They comprise about 1% soluble protein in the brain (6).

There are 7 highly homologous isoforms in mammals, namely β , γ , ϵ , σ , ζ , τ and η (7). 14-3-3s are highly conserved proteins. There are 2 isoforms in yeast and drosophila, and there are 15 isoforms in plants. The *Saccharomyces cerevisiae* isoform BMH1 share ~70% amino acid sequence homology with mammalian 14-3-3 ϵ isoform. This similarity strongly suggest high degree of functional conservation (8).

1.3b Function discovery

It was not until 20 years after the initial discovery, was the first function of 14-3-3 discovered as an activator of tryptophan and tyrosine hydroxylases which is necessary for dopamine synthesis and other neurotransmitters (9).

14-3-3 binds to a variety of target proteins many of which are involved in cancer including receptors like IGF1R(10, 11), kinases like Raf-1 (12-17) and

Bcr (18), docking molecules like insulin receptor substrate I (IRS-1) (19) and p130^{Cas} (20), phosphatase like Cdc25 (21), death regulator like Bad (22), and oncogene products like Polyoma-virus middle tumor antigen (PyMT) (23) and Bcr-Abl (18), which indicated that 14-3-3 could be potential oncogene (24). These findings of 14-3-3s interaction with different targets in biochemical and genetic screenings reflected the physiological importance of 14-3-3s in diverse cellular pathways (8).

As 14-3-3 lack endogenous enzymatic activity, it was thought to be allosteric cofactor or molecular chaperone to affect the target proteins enzymatic activity, subcellular localization, protein stability, interaction with other molecules and post-translational modification (4).

1.3c Target interaction

Although 14-3-3 can bind to the target proteins independent of phosphorylation, 14-3-3 binds to their ligands mainly in a phosphorylation dependent manner. 14-3-3 is the first protein family that binds to specific phospho-serine/threonine containing motif (25, 26). By screening oriented peptide library, two consensus motifs were found to interact with 14-3-3, RSXpSXP (mode 1) and RXXXpSXP (mode 2), where pS represents phosphoserine (27, 28).

1.3d Structure basis

14-3-3s are highly homologous in their amino acid sequence (8). It is predicted that each isoform may have specific functions. However, the structure studies did not support this hypothesis. 14-3-3 isoforms are highly similar in their dimeric structure (27-30). Crystal structure indicated that 14-3-3 forms heterodimer or homodimer in cells. The 14-3-3 ζ dimer is in a flattened horseshoe shape. Each monomer contains 9 α -helices that are organized in an anti-parallel manner. The first 4 helices are necessary to form the dimer. The helices-3, 5, 7, 9 composed a conserved amphipathic binding groove(29) . This structure is conserved in all 14-3-3 isoforms (28). (Figure 2, 3)

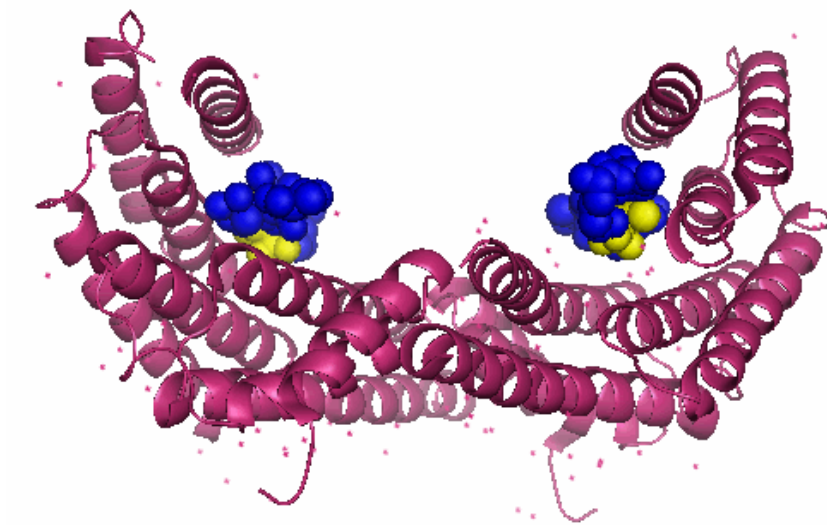


Figure 2. Crystal structure of 14-3-3 ζ dimer. The red part indicates 14-3-3 ζ structure. The blue part indicates the 14-3-3 binding motif in integrin beta2 variant chain. The yellow part indicates the phosphorylated threonine site. Diagram generated by PyMOL software using PDB ID# 2V7D

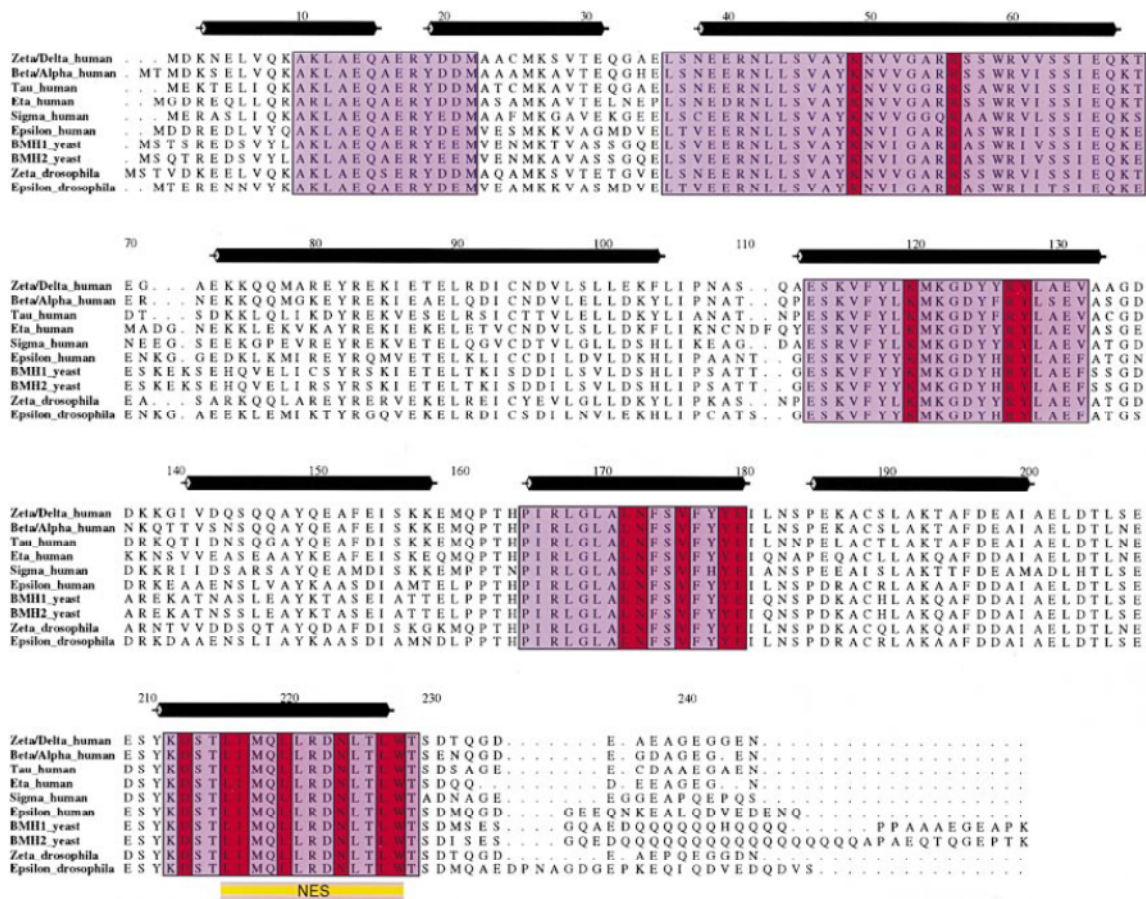


Figure 3. 14-3-3s share high similarity in their amino acid sequence and crystal structure. Ten 14-3-3 proteins from different species were aligned with CLUSTAL algorithm. α -helices are indicated above the sequence using black rectangles. Nucleus exportation signal sequence was colored in yellow below the sequence. 5 blocks with highest sequence homology are shaded in purple and the residues responsible for direct target binding are shaded in red.

1.3e Regulation of 14-3-3

The isoform specific functions of 14-3-3s could be achieved by at least 3 ways, strict regulation of cell type specific isoform expression, post-translational modification and regulation of the availability (8, 24). The brain constitutively expresses most 14-3-3 isoforms, whereas the other tissues express mainly one or another isoform (31-33). 14-3-3 can be phosphorylated at S58 (34), S184 (35) and T232 (36). These phosphorylation either inhibited the dimerization of 14-3-3 monomers or inhibited 14-3-3 binding to the target proteins, which inhibited 14-3-3 function. The cell can also express fluctuated level of 14-3-3 ligands, thus competitively regulating the availability of 14-3-3 to other target proteins.(37-39)

1.3f Specificity function of 14-3-3 isoforms

Recent studies have revealed that each 14-3-3 isoform preferentially binds to their target proteins and is involved in different biological processes and human diseases. 14-3-3 σ has been known to stabilize p53 and hence suppresses tumor growth (40-42) and is frequently lost in cancer (43-46). 14-3-3 σ also binds to Par3 and regulate cell polarity (47). 14-3-3 ϵ binds to TGF β RI thereby enhancing TGF- β signaling (48). 14-3-3 ϵ can also bind to PolyA polymerase and regulates its cellular localization (49). Loss of 14-3-3 ϵ in mouse models results in embryonic lethality and haplo-insufficiency leading to neuronal development defects which mimics the human Miller-Dieker Syndrome (MDS) (50). 14-3-3 γ binds to PKC and regulates PDGF signaling in vascular smooth muscle cells (51). Mice with targeted deletion of 14-3-3 γ did not show any

obvious phenotype (52). 14-3-3 τ regulates E2F stability and is required for autophagy (53). 14-3-3 τ knockout mice were embryonic lethal. 14-3-3 τ heterozygous mice were haploinsufficient and were sensitive to myocardial infarction (54).

So although 14-3-3 isoforms are highly homologous and structurally similar to each other, they have different function both *in vitro* and *in vivo*.

1.4 14-3-3 ζ

1.4a 14-3-3 ζ in human diseases

Among all the 14-3-3 isoforms, the 14-3-3 ζ (zeta) has been demonstrated to be involved in several human diseases, like Creutzfeldt-Jakob Disease (CJD) (55), Alzheimer Disease (33, 56), progressive multifocal leukoencephalopathy (PML) (57), atherosclerosis (58), Huntington disease (59) and especially multiple cancer types including lung (60, 61), breast (62, 63), ovarian (64), head and neck (65), oral cancers (66) and lymphomas (67). These data support the idea that 14-3-3 ζ is critical in human diseases. However, how exactly 14-3-3 ζ functions in these diseases remain to be explored. Studying the role of 14-3-3 ζ could provide new opportunities to develop better therapy and potentially benefit the patients. It is urgent to develop animal model in which 14-3-3 ζ expression could be manipulated to study the role of 14-3-3 ζ *in vivo*. Unfortunately no such animal models have been reported and available to the field so far.

1.4b 14-3-3 ζ in breast cancer

14-3-3 ζ isoform is. It is located on chromosome 8q22 which is frequently amplified in breast cancer (68). We and others have shown that 14-3-3 ζ is overexpressed in ~45% breast cancer patients mainly due to amplification which predicts poor clinic outcome (62). Overexpression of 14-3-3 ζ resulted in chemotherapy resistance in breast cancers (68). 14-3-3 ζ activates Akt, suppresses p53 and hence rendering the cells resistant to apoptosis (69). 14-3-

3 ζ can bind to TGF β RI, stabilize it and promotes epithelial-to-mesenchymal transition (EMT). It also cooperates with ErbB2 to promote early stage breast lesion to invasive breast cancer (63). All these data suggest that 14-3-3 ζ plays important role in breast cancer. 14-3-3 ζ can be a potential therapeutic target in breast cancer and other cancer types (70)

1.5 MicroRNA-126

MicroRNAs are a class of ~22 nucleotide noncoding RNAs that regulate gene expression by either promoting mRNA degradation or repressing protein translation (71). Hundreds of microRNAs have been identified in human and other eukaryotes. Many of them are transcribed from introns of protein coding genes or intergenic sequences. MicroRNAs are initially transcribed as large pri-microRNAs in the nuclear. After cleavage by Drosha complex, pre-microRNAs will be generated and translocated into the cytoplasm. Then the ribonuclease Dicer and its cofactors will process the precursors into 19-25nt microRNA duplexes. The microRNA heteroduplex will incorporate into RNA-induced silencing complex (RISC) where the microRNAs could target specific mRNA through complementary binding to the 3'-UTR region. In animals the 5' proximal "seeding" sequences (nucleotide 2 to 8) appear to be the major determinant of paring specificity (72, 73). More than one-third human genes could be regulated by microRNAs (74). The opposite strand known as star (*) strand is generally degraded. In this way MicroRNAs regulate a wide variety of biological processes (75).

MicroRNA-126 is located in the intron 7 of EGFL7 gene (76). It will transcribe into 2 mature miRNAs, miR-126 and miR126*. MiR-126 expression was detected in all tissues with the highest in heart and lung. MiR-126 is an endothelial specific microRNA that regulates vascular integrity and angiogenesis (76-78). Targeted

deletion of miR-126 resulted in lethality and lung deflation along with vascular leakage, edema and hemorrhaging (76).

MiR-126 has been reported to involve in several human diseases such as type II diabetes (79), malaria (80), coronary artery disease (81) cystic fibrosis (82) and cancer (83-86). Its role in cancer has remained controversial and need to be elucidated in the future (87).

Rationale, Purpose and Significance

According to the previous introduction, I hypothesized that 14-3-3 ζ plays an important role in breast cancer formation and progression. Better understanding the role of 14-3-3 ζ in breast cancer could help us understand this disease better. I would like to test this hypothesis in a genetically engineered mouse (GEM) model which could collectively demonstrate breast cancer biology *in vivo*.

Our lab previously found that knocking down 14-3-3 ζ using siRNAs sensitized breast cancer cells to stress induced apoptosis without affecting its most homologous isoform, 14-3-3 β (62), which suggested that 14-3-3 ζ had specific important functions that could not be compensated by other 14-3-3 isoforms.

14-3-3 ζ gene is located on mouse genome chromosome 15 without any other known genes or non-coding RNAs located inside or close to that region, which made the knockout of 14-3-3 ζ feasible. Any phenotype observed in the 14-3-3 ζ gene knockout mouse is likely to be specific to loss of 14-3-3 ζ alone.

So I decided to generate a 14-3-3 ζ knockout mouse strain, in which I could study the function of 14-3-3 ζ *in vivo*. Meanwhile I could initiate to test whether 14-3-3 ζ could be a cancer therapeutic target. This study could potentially benefit a big proportion of patients who had aberrant regulation of 14-3-3 ζ .

Chapter 2 Material and Methods

2.1 14-3-3 ζ knockout Mice Generation and Maintenance

ES cell line RRR334 was obtained from Mutant Mouse Regional Resource Center (MMRRC). RT-PCR was performed to confirm that the cell line inactivates 14-3-3 ζ . The primer sequence for the exogenous was forward: 5'-TGCTGAGAAAAAGCAGCAGA and reverse: 5'-GACAGTATCGGCCTCAGGAAGATCG. The primer sequence for endogenous 14-3-3 ζ ctrl PCR was forward: 5'-TGCTGAGAAAAAGCAGCAGA and reverse: 5'-TTGTCATCACCAGCAGCAAC. Genetic Engineered Mouse Facility at MD Anderson Cancer Center injected the cells into C57Bl/6 albino blastocysts. The chimera mice were mated with C57Bl/6 albino mice to test germline transmission and get 14-3-3 ζ knockout founder mice. The primer sequences for PCR genotyping were forward: 5'-CAACCATGTTGGGATAGAGG homologous to 14-3-3 ζ intron 3, reverse: 5'-CCAAATAAGCCTTCCCTTCC homologous to intron 3 and 5'-AAGGGTCTTTGAGCACCAGA homologous to the gene trap vector. The PCR will generate a 954bp fragment from the wild type allele and a 544bp fragment from the mutant allele. Mice were backcrossed into C57Bl/6, FVB/N congenic background or outbred to CD-1 genetic background respectively and maintained since then. The C57Bl/6J and FVB/NJ mouse breeders were purchased from the Jackson Laboratory, Bar Harbor, Maine. The CD-1 breeders were purchased from Charles Rivers, Wilmington, MA.

2.2 Mammary Gland Whole Mounts

The number 4 mammary glands on the left side of the mice were spread onto microscopic slides, fixed in Carnoy's fixative overnight, hydrated and stained with carmine alum stain (Sigma, St. Louis, Mo) overnight, and were then dehydrated through sequential ethanol, treated with xylene to remove fat, and mounted with Secure Mount (Fisher Scientific, Pittsburgh, PA) and cover slips. Mammary gland tissue samples were collected during all phases of the estrous cycle. The samples were imaged using Zeiss Discovery V20 dissection microscope and axiom imaging software that came with the microscope.

2.3 Tissue Collection and Histological Analysis

The mouse embryos were collected by C-section at 18.5dpc. The lung tissues were collected after euthanasia following IACUC.

Mammary tumor formation was monitored by palpation twice a week. Upon formation of a palpable tumor, the mice were observed for 3-4 weeks for tumor progression. When the tumor diameter reached 15mm, the mammary tumors and lungs were harvested. Excised lungs were examined for grossly detectable lesions.

Tissues were fixed in 10% neutral buffered formalin for 12-18 h. The samples were stored in 70% ethanol, and then embedded in paraffin. Paraffin sections of 5µm were stained with hematoxylin and eosin. Mammary tumor histology and lung metastasis were independently evaluated by two pathologists (Y.X and

H.W). Immunohistochemistry (IHC) was performed as previously described (63). Antibodies used are Ki67 (DAKO, Carpinteria, CA M7249), Tunel (Roche, Indianapolis, IN), CD34 (eBioscience, San Diego, CA 14-0341), 14-3-3 ζ (C-16, Santa Cruz, Santa Cruz, CA sc-1019).SP-A (Santa Cruz sc-13977), AQP5 (Calbiochem, Germany 178615). For IHC analysis and quantification, 10 fields were randomly chosen at 200X magnification. The total number of cells and positive cells were counted and the average percentage of positive cells was determined.

2.4 Immunoblotting

Tissues and mammary tumors were collected from mice. Protein extracts were made by homogenizing samples in tissue lysis PBSTDS buffer [10 mmol/L sodium phosphate (pH 7.3), 154 mmol/L NaCl, 5% sodium deoxycholate, 1% SDS] using a tissue grinder, followed by centrifugation to remove particulate matter and lipids. Immunoblotting was performed as previously described (63). Antibodies used are anti-HA high affinity (clone 3F10, Roche 11867423001), 14-3-3 ζ (C-16, Santa Cruz sc-1019), Neu (C-18, Santa Cruz sc-284), Erk (Cell Signaling 4695), pErk (T202/Y204, Cell Signaling 4370), Mek1 (Cell Signaling 9126), pMek1 (S221, Cell Signal 2338), Akt (Cell signaling 9272), pAkt (S473, Cell signaling 3787), p53 (DO-1, Santa Cruz sc-126), Bax (B-9, Santa Cruz sc-7480), VEGF (A-20, Santa Cruz sc-152), PyMT(Novus Biologicals NB100-2749), β -actin (Sigma A5441), α -tubulin (Sigma T5168), HIF1- α (Novus Biologicals NB100-105) and IGF1R- β (Cell Signaling 3027)

2.5 Quantitative RT-PCR for microRNA quantification

RNA of the tissue samples was retrieved using Trizol (Invitrogen, Carlsbad, CA) following the standard protocol. Reverse transcription was performed using Taqman MicroRNA Reverse Transcription kit (Applied Biosystems 4366569) and real time PCR was performed using Taqman Universal PCR Master Kit (Applied Biosystems 4324018) and iQ SyBR Green Supermix (Bio-Rad 170-8882). The specific primers and probe for miR-126 RT-PCR was purchased from Applied Biosystems, 4427975-002228. The real time PCR was done on Bio-Rad iCycler Real Time PCR machine. The primer sequences for CD31 are forward: 5'- CTGGTGCTCTATGCAAGCCT and reverse: 5'- AGTTGCTGCCCATTTCATCAC. The primer sequences for 18S ribosome protein are forward: 5'- AACCCGTTGAACCCCATC and reverse: 5'- CCATCCAATCGGTAGTAGCG.

2.6 Transwell migration assay

3×10^4 mouse endothelial cells resuspended in 500ul serum free medium were seeded in the top chamber of the 24-well 8-um pore transwell plates. 600ul 10% FBS containing medium was used as chemo-attractant in the bottom chamber. The plates were incubated at 37C for 4 hours. The cells were fixed in 10% neutral buffered formalin for 1 hour and stained with 0.5% crystal violet for 1 hour. The plates were flushed under tap water to remove excessive dye. The cells that did not migrate were removed by cotton tips. Images were taken with

Zeiss Discovery V20 microscope with equipped software. Quantification of the migrated cells was performed using Adobe Photoshop and ImageJ software.

2.7 Tube formation assay

Matrigel (BD, Franklin Lakes, NJ 356231) was thawed at 4C overnight before assay. 500ul matrigel was added into each well of the 24-well plate. The plates were incubated at 37C 30 minutes to 1 hour to form gel. 3×10^5 cells resuspended in 10% FBS containing DMEM/F-12 medium were plated above the matrigel and incubated for 6 hours at 37C. Tube formation of the endothelial cells was imaged with Olympus inverted fluorescence microscope and quantified using ImageJ software.

2.8 Assessment of Proliferation, Apoptosis, and Angiogenesis

To assess proliferation rate or apoptosis, 1000 tumor cells were counted for the percentage of Ki67 or TUNEL positive-staining cells by investigators blinded to the identity of the mice. Angiogenesis was evaluated by CD34 IHC staining and by counting blood vessels in three areas of the section at 200X magnification. The blood vessel index was expressed as the mean number of vessels in the three areas.

2.9 Growth Hormone Measurement

Blood samples were extracted through tail vein from 4 week old mice of both sexes. Blood samples were placed on ice 2h to allow aggregation. Centrifuge

the samples at 1500g for 10 minutes. Collect the top clear part of serum. Mouse circulating growth hormone was measured using ELISA kit (Diagnostic Systems Laboratories, Webster, TX DSL-10-72100) following the product instruction.

2.10 Circulating IGF-1 Measurement

Mouse circulating IGF-1 was measured using RIA kit (Diagnostic Systems Laboratories DSL-2900) following the product manual.

2.11 Blood Glucose Measurement

A drop of blood was retrieved from a tail snip. Blood glucose level was measured using Roche AccuChek Aviva blood glucose test system. Blood drawing was performed *ad libitum*.

2.12 Glucose tolerance assay

Age matched mice with different genotypes were fasted for 16 hours. Roche AccuChek Aviva blood glucose test system was used to measure blood glucose level of the mice. Basal blood glucose was measured using the blood retrieved from the tail snips and was set as time point of 0 minute. 3g/kg weight of glucose was injected intraperitoneally. Blood glucose was measured at the time points of 15, 30, 60 and 120 minutes after injection.

2.13 Glucose uptake measurement

Mice were injected (i.v.) 100 μ l of 2-NBDG (50 μ M) and sacrificed 30 minutes later. Their livers and brains were collected and imaged by Maestro Imaging System (CRi Inc.) to measure 2-NBDG uptake *in vivo*. Fluorescence intensity was measured using ImageJ software.

2.14 Statistical Analyses

Analysis of mammary tumor latency was performed using the Kaplan-Meier method. Differences in survival were determined using log-rank test. Other statistical differences were assessed with Student's t-test or one-way ANOVA. A *P*-value of <0.05 was considered statistically significant.

Chapter 3 Results and Discussion

3.1 Generation of 14-3-3 ζ knockout mouse

3.1a Generation of 14-3-3 ζ mutant mouse strain

To systematically study the role of 14-3-3 ζ *in vivo*, I generated a 14-3-3 ζ knockout mouse strain by gene trap. The cell line RRR334, in which 14-3-3 ζ was inactivated according to the 5'RACE data from Baygenomics database, was obtained from the Mutant Mouse Regional Resource Center (MMRRC). We confirmed silencing of 14-3-3 ζ in the cell line by RT-PCR using a forward primer homologous to exon 3 and a reverse primer homologous to β -geo cassette in gene trap vector, pGT0Lxf, followed by sequencing the PCR product (Figure 4). By designing multiple forward primers homologous to intron 3 and PCR amplification along with a reverse primer homologous to gene trap vector, I identified the exact integration site of the gene trap vector in 14-3-3 ζ gene. The first 152 base pairs (bp) of the gene trap vector were lost during integration. The integration site of the gene trap vector was located about 3351bp downstream of exon 3 as determined by PCR and sequencing the PCR product (Figure 5). Southern blot was also designed and performed to confirm the genomic integration. PCR genotyping primers were designed based on the integration site (Figure 6). The ES cells were injected into C57Bl/6 albino mouse blastocysts by the Genetic Engineered Mouse Facility (GEMF) at MD. Anderson Cancer Center. Chimera mice with high ES cell contribution based on their fur color were mated with C57Bl/6 albino mice to determine germ line transmission

and obtain 14-3-3 ζ knockout founder mice. Founder 14-3-3 ζ heterozygous (+/-) male with (+/-) female mice were mated to generate 14-3-3 ζ homozygous (-/-) mutant mice.

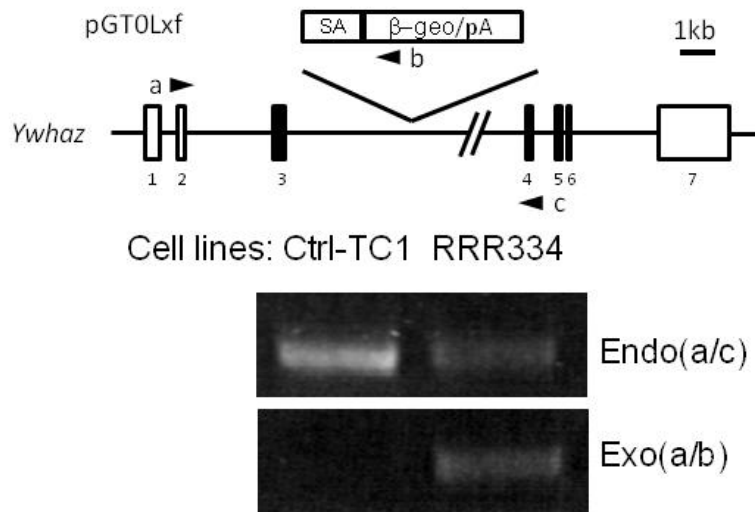


Figure 4. RT-PCR confirmation that the ES cell line RRR334 had 14-3-3 ζ inactivated. Schematic view of that the gene trap vector integrated into the intron 3 of 14-3-3 ζ gene. Ywhaz is the HUGO Gene Nomenclature Committee approved gene symbol for 14-3-3 ζ . The line indicates the introns for 14-3-3 ζ gene, whereas the rectangles indicate the exons. The solid parts indicate the coding region for 14-3-3 ζ protein. The gene trap vector pGT0Lxf was integrated ~3.3kb downstream of exon 3. SA is short for the splice acceptor sequence of mouse En2 exon 2. β -Geo/pA indicates the fusion of β -galactosidase and neomycin transferase followed by SV40 polyadenylation signal. The arrows indicate the primers for RT-PCR. The scale bar is for 1kb length of DNA sequence. The endogenous 14-3-3 ζ is expressed both in wild type ES cell control, TC1 and the mutant cell line RRR334. The exogenous mutant allele only exists in the RRR334 cell line.

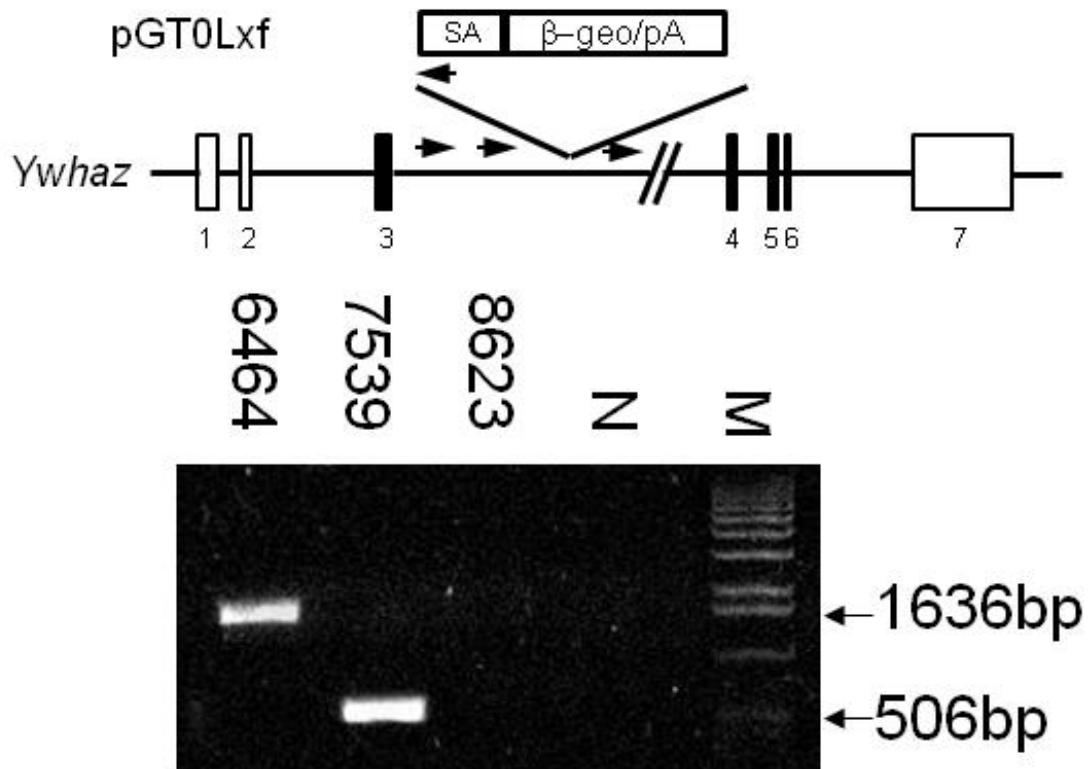


Figure 5. Determination of the gene trap vector integration site in 14-3-3 ζ genome using PCR. The integration of the gene trap vector into 14-3-3 ζ gene is described earlier. The arrows indicate the primer for PCR. The numbers on each lane of the gel indicate the primer position in the 14-3-3 ζ gene. "N" is for negative control and "M" is for marker. The 1636bp and 506bp maker sizes are shown.

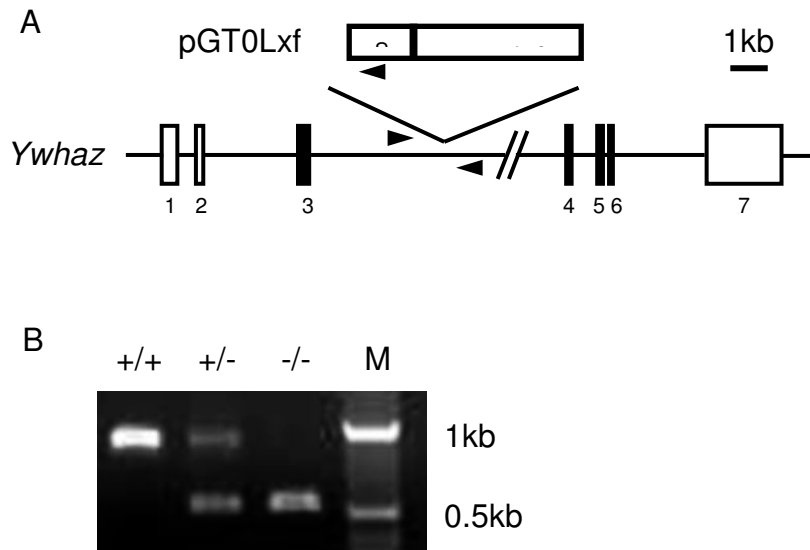


Figure 6. Genotyping of 14-3-3 ζ mutant mouse. A. schematic view of the integration of the gene trap vector into 14-3-3 ζ gene as described earlier. Arrow heads indicate the primers for genotyping. B. Representative data of PCR genotyping of 14-3-3 ζ wild type (+/+), heterozygous (+/-) and homozygous mutant (-/-) mouse. "M" is for DNA marker. 1kb and 0.5kb DNA fragments were indicated as shown. Wild type allele generated a 954bp band and the mutant allele generated a 544bp PCR product.

3.1b This mouse strain is a strong hypomorphic mutant model for 14-3-3 ζ

14-3-3 ζ expression was significantly inhibited in multiple tissue types from the knockout mice, especially in mammary gland to our interest (Figure 7). As the exon 3 which encodes the first 98 amino acid was expected to be expressed as a fusion protein followed by the β -geo cassette, I tested whether the N-terminal part of 14-3-3 ζ protein had any function. We transfected the HA-tagged N-terminal 145 amino acids of 14-3-3 ζ which encodes a shortened 14-3-3 ζ form lacking the C-terminal target binding groove structure (29, 30) and should be similar with the N-terminal 98aa 14-3-3 ζ fragment in term of structure, into MCF7 cells. I found that the protein was barely detectable by western blot using HA antibody. Only when the cells were treated with the proteasome inhibitor MG132 could we detect the expression of the HA tagged protein. I could not detect the 14-3-3 ζ / β -geo fusion protein in mouse tissues by western blot using either 14-3-3 ζ or β -gal antibody. There was no difference in proliferation as determined by MTT assay. The activation of Ras/Raf/Erk and PI3K/Akt signaling, as indicated by phosphorylated Mek1 and Akt, which could be activated by overexpression of 14-3-3 ζ (12, 88), were not affected (Figure 8). It is also reported that C-terminal deleted 14-3-3 could not bind to hTERT and promote its nuclear translocation (89). Based on these, I conclude that the N-terminal part of 14-3-3 ζ is not functional probably due to its rapid degradation. Considering all these data, this mouse strain is a strong hypomorphic mutant model in which we can study the role of 14-3-3 ζ *in vivo*.

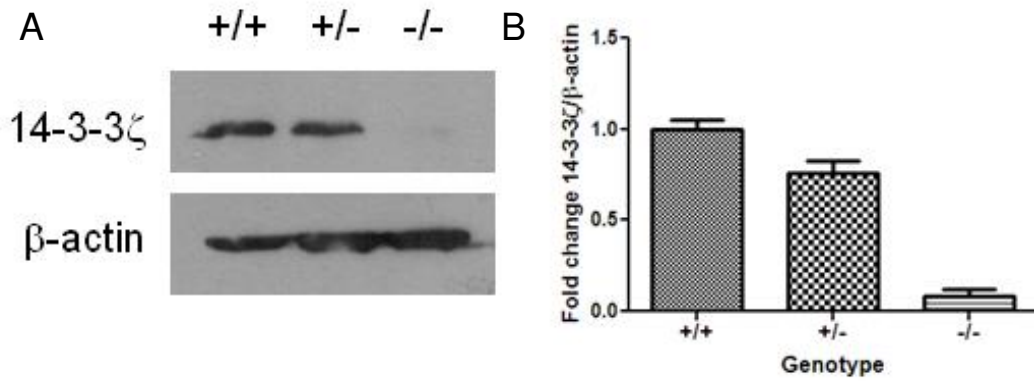


Figure 7. 14-3-3 ζ is significantly downregulated in homozygous mutant mouse mammary gland. A. Western blot to detect 14-3-3 ζ expression in wild type (+/+), heterozygous mutant (+/-) and homozygous mutant (-/-) mouse mammary gland. β -actin was used as loading control. B. Quantification of 14-3-3 ζ expression in different genotyping mice tissues from 3 independent experiments.

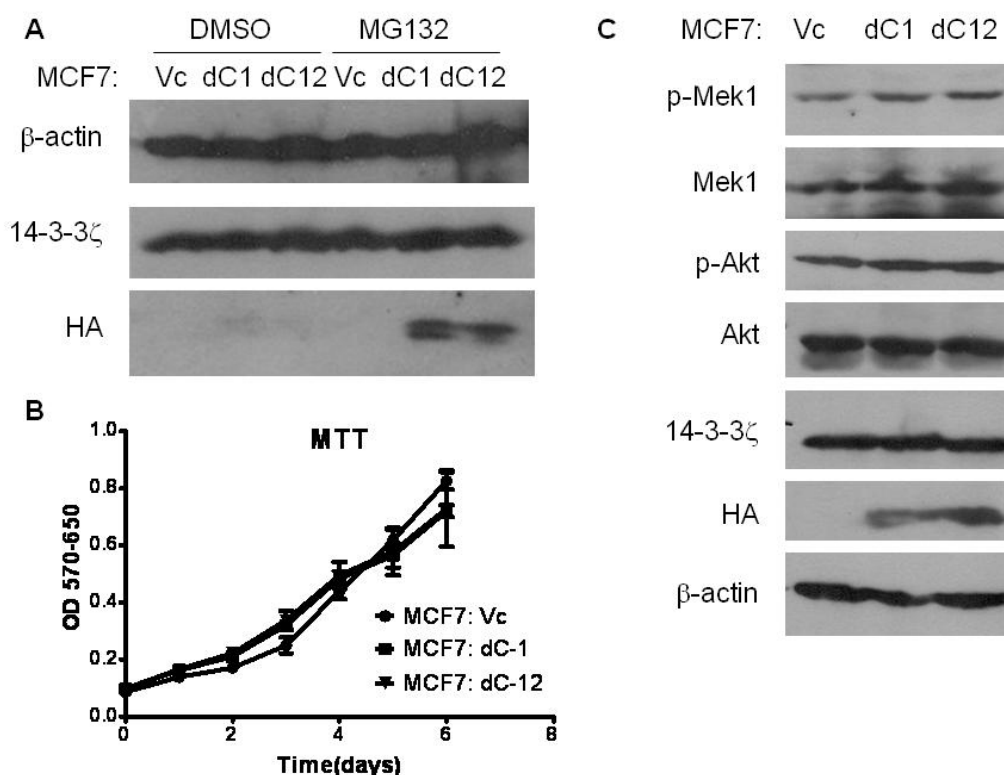


Figure 8. 14-3-3ζ N-terminal fragment is non-functional. A. 14-3-3ζ N-terminal fragment was not stable. Western blot of lysate from MCF7 transfected with vector control (Vc) and 2 HA-tagged delta-C-terminal fragment of 14-3-3ζ transfected cell lines (dC1 and dC12) treated with DMSO or 50nM MG132 for 4 hours. Endogenous 14-3-3ζ was detected using 14-3-3ζ antibody while the exogenous 14-3-3ζ fragment was detected using HA antibody. β-actin was used as loading control. B. 14-3-3ζ N-terminal fragment did not affect proliferation in MCF-7 cells suggested by MTT assay. OD was measure at 570nm and normalized to 650nm. C. 14-3-3ζ N-terminal fragment did not activate Mek1 and Akt indicated by their phosphorylation status. β-actin was used as loading control

3.1c Discussion

The strategy I used to knockout 14-3-3 ζ was gene trap. Gene trap is a high-throughput method to inactivate specific gene expression by introducing insertional mutations genome wide. In addition to the traditional loss of function mutant alleles introduced, recently developed gene trap vector also allowed a variety of post-insertional modification strategies for the generation of other experimental alleles. It is a very valuable resource for the research community to study specific gene function *in vivo*. For more details about how gene trap works, one can go to the International Gene Trap Consortium at www.igtc.org for more information.

Despite of all the advantages gene trap provides, it has intrinsic limitation and pitfalls as well. I had two concerns. First, gene trap utilized strong splicing acceptor site to make alternative RNA splicing product in competition to the endogenous gene. It is highly possible that the endogenous gene was still expressed at certain extent. The dosage of the leakage may be critical for any phenotype I would observe. Secondly, gene trap of the host gene will result in a fused mRNA product composed of the exons in front of the gene trap insertion site and the β -geo cassette. If the exons encode protein sequences, it is necessary to confirm that part of the protein is not functional. Any retain of function, gain of function, dominant negative would interfere the interpretation of the data we generate from the mouse.

Here I experimentally showed that endogenous 14-3-3 ζ expression is significantly downregulated in the knockout mouse tissues and the N-terminal part of 14-3-3 ζ is not functional. Only ~5% 14-3-3 ζ was expressed compared to the wild type mouse tissues. The remaining 14-3-3 ζ protein probably cannot play full function as that in the wild type mouse tissues. With these data in hand, I can be confident to move on to test the phenotype mediated by loss of 14-3-3 ζ .

3.2 14-3-3 ζ knockout mice are lethal neonatally

3.2a 14-3-3 ζ mutant mice are lethal neonatally in C57Bl/6 genetic background

An interesting phenotype was observed after mating the founder mice and that is only about 5% of the offspring generated from mating heterozygous male and female founders were 14-3-3 ζ homozygous mutant mice as determined by PCR genotyping 10 days after birth (table 1). This indicates that 14-3-3 ζ knockout mice may be lethal during embryo development or quickly after birth.

As about 5% homozygous mice survived, the genetic background is likely to play important role mediating the lethality phenotype. To test this, I backcrossed the mutant to strain into congenic C57Bl/6 genetic background determined by genome scan using a panel of simple sequence length polymorphisms (SSLP) (microsatellites) markers. No homozygous mutant pups were found at the time of genotyping 10 days after birth (table 1), which confirmed the lethality phenotype we observed in B6/129P2 hybrid genetic background. The lethality is even more severe in this genetic background. To determine the time point when the 14-3-3 ζ knockout embryos die, we dissected the embryos at 18.5dpc. We observed that the ratio of the knockout embryos matched the Mendelian Inheritance Law, which indicated that the 14-3-3 ζ knockout embryos were alive at this time point (table 1). In contrast to that the wild type and heterozygous embryos that started to breathe, became red and survived after dissection, the knockout embryos got pale and died quickly after dissection after several

attempts to breathe. Similar phenomenon was observed in new born mice, which suggested that the 14-3-3 ζ knockout mice are lethal neonatally in C57Bl/6 genetic background.

Strain/genotype	+/+	+/-	-/-	P-value
B6/129P2 F2	22	39	3	0.0052**
B6 congenic	58	72	0	<0.0001***
B6-18.5dpc	16	32	15	0.9879
CD-1	36	73	38	0.9849

Table 1. 14-3-3 ζ knockout mouse are lethal neonatally in C57Bl/6 genetic background and are viable in CD-1 background. Genotyping of pups generated from mating heterozygous breeders was performed 10 days after birth. Genotyping of the embryos were dissected at 18.5dpc (days postcoitus). B6 indicates the C57Bl/6 strain. 129P2 was previously name as 129/OlaHsd in which background the ES cells were originally generated.

3.2b 14-3-3 ζ mutant pups die due to respiratory failure

All the 14-3-3 ζ knockout embryos die within 0.5 hour after dissection indicating that they may die from breathing distress (90). To test this, we dissected the lungs of the embryos. In contrast to the wild type lungs which floated in water, the knockout lungs sank, suggesting no air got into the lungs. The same phenomenon was also observed in new born knockout pups. So it is concluded that the 14-3-3 ζ knockout mice are lethal neonatally due to respiratory failure.

H&E staining of the lung section indicated that the knockout mice had defects in lung development and was stuck at the pseudoglandular stage. The lungs lacked saccular structure and had increased mesenchymal compartment and thickened saccular septae (Figure 9). To better understand the pathology in the knockout lungs, we performed immunohistochemistry staining on the lung sections. There was no difference in proliferation as determined by Ki67, type I and type II pneumocyte differentiation determined by pulmonary surfactant-associated protein A (SP-A) and Aquaporin isoform 5 (AQP5) staining (Figure 10). Interestingly, we found that the blood vessels in the knockout lungs were not integrated. Around the vessels, there were aggregations of leukocytes. Meanwhile there were increased blood cells in the knockout lung section compared to the wild type counterparts. These data suggest that defects in angiogenesis play an important role mediating the breathing distress in the knockout mice (Figure 11).

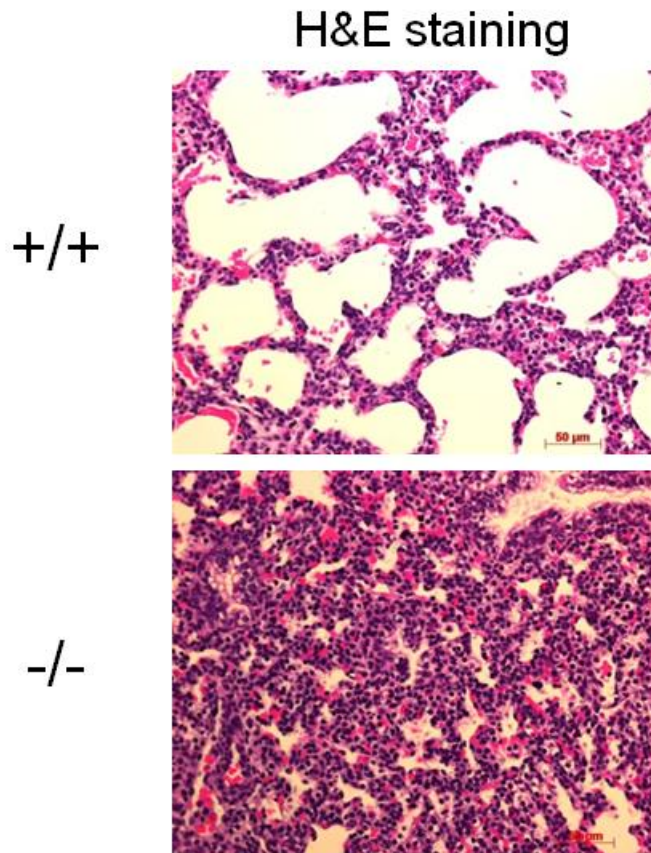


Figure 9. 14-3-3 ζ knockout mice had defect in lung development. Hemotoxylin and Eosin staining was performed on lung tissue dissected from 18.5dpc embryos. The wild type lungs were inflated and had saccular structure. The 14-3-3 ζ knockout lungs were deflated, lack saccular structure and had thickened septae, increased mesenchymal compartment and more blood cells spread in the lung tissues. Scale bar indicates 50um in length

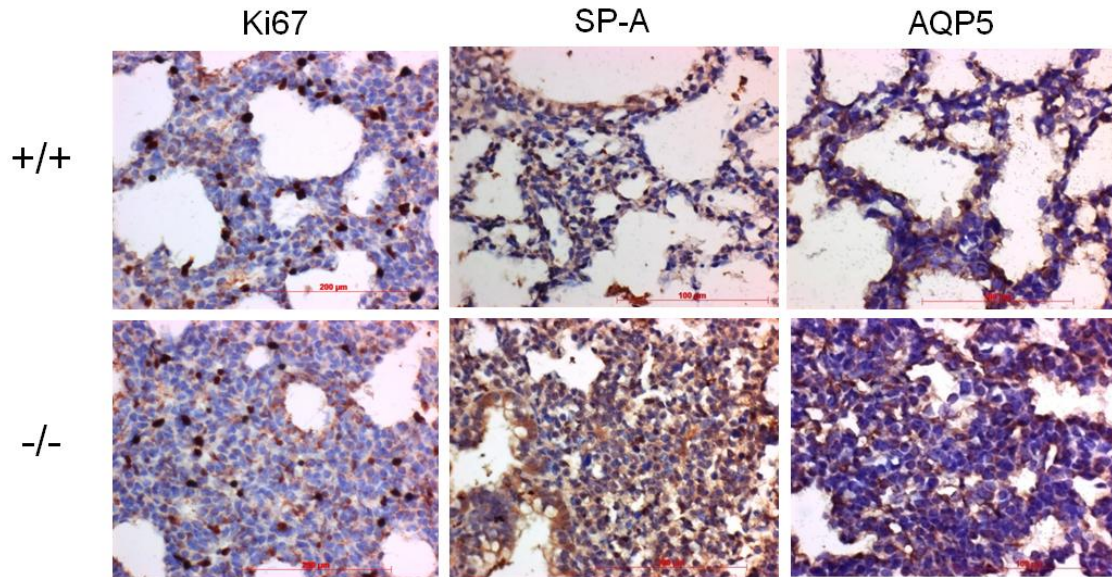


Figure 10. 14-3-3ζ did not affect proliferation and pneumocytes differentiation. Immunohistochemical staining of proliferation marker Ki67, type I pneumocyte marker SP-A and the type II pneumocyte marker AQP5 were performed on lung tissue sections from wild type (+/+) and 14-3-3ζ homozygous mutant (-/-) 18.5dpc embryos. Scale bar indicates 200um in length.

CD34

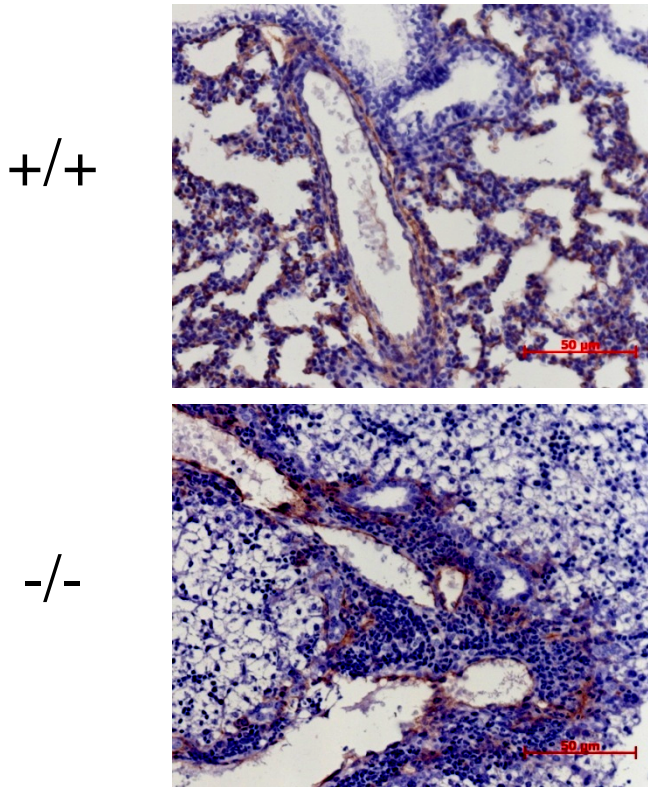


Figure 11. Loss of 14-3-3 ζ lead to angiogenesis defect in lungs. Blood vessel endothelial cell marker CD-34 was stained immunohistochemically on 18.5dpc embryos lungs. 14-3-3 ζ knockout lungs had leaky bid blood vessels and fewer peripheral blood vessels. Aggregation of leukocytes was present around the broken vessels in 14-3-3 ζ knockout lungs. Scale bar indicates 200um in length.

3.2c microRNA-126 is downregulated in 14-3-3 ζ knockout lungs

To understand the key molecular mechanism mediating respiratory distress, I searched the Mouse Genome Informatics (MGI) database on the Jackson Laboratory using key word “lethal”, “respiratory” and “angiogenesis”. More than 100 genes popped out, among which a lot are 14-3-3 ζ binding proteins like Tgf β RI, β -catenin. Interestingly, microRNA-126 is the only microRNA in the list.

MiR-126 is an endothelial specific microRNA that regulates vascular integrity and angiogenesis (76-78). Targeted deletion of miR-126 resulted in lethality and lung deflation due to vascular abnormalities. The angiogenic signaling was significantly diminished in the knockout tissues and resulted in defective endothelial sprouting, adhesion and growth (76). MiR-126 was upregulated by ~ 3 fold in our 14-3-3 ζ overexpression cell line compared to the vector control cell line as determined by a microRNA microarray.

I extracted RNA from the lung tissue and performed real-time quantitative reverse-transcript polymerase-chain reaction (qRT-PCR) and found that the miR-126 level was significantly downregulated in the 14-3-3 ζ knockout lungs comparing to the wild type counterparts (Figure 12).

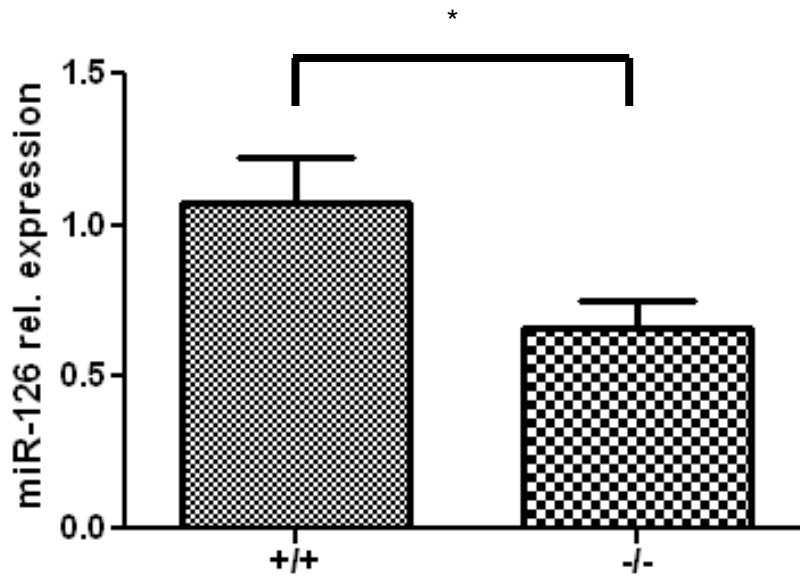


Figure 12. MicroRNA-126 was downregulated in 14-3-3 ζ knockout lungs. Total RNA was extracted from 18.5dpc lung tissues from wild type (+/+) and 14-3-3 ζ knockout (-/-) embryos. MiR-126 expression level was determined by quantitative real-time RT-PCR normalized to PECAM1 mRNA level.

3.2d Discussion

Here I observed the neonatal lethality in 14-3-3 ζ knockout mouse under C57Bl/6 genetic background.

Genetic background apparently play important role mediating this phenotype, as several 14-3-3 ζ knockout mice survived at the time of genotyping which is 10 days after birth. Combining with the data later in part 3.3, the knockout mice are completely viable and fertile in CD-1 and FVB/N genetic background. One possible reason may be that different strains have different alternative splicing capability. The 14-3-3 ζ expression level may be much lower in the B6 genetic background. My data did not support this view. The expression level of 14-3-3 ζ remained low in all the genetic background. This leads to another possible explanation that 1 or more C57Bl/6 specific mutations in addition to loss of 14-3-3 ζ resulted in the lethality. It will be interesting to study which genes they are. If someone is to develop 14-3-3z targeting therapy for patients, it is important to identify and exclude those patients bearing such mutation from the therapy to prevent severe side effects.

MiR-126 downregulation correlated with the 14-3-3 ζ loss mediated lethality. However, miR-126 was only downregulated about half in 14-3-3 ζ knockout mice lungs. MiR-126 heterozygous mutant mice were viable and fertile. Also 14-3-3 ζ knockout mouse did not completely phenocopy the miR-126 knockout mouse. So downregulation of miR-126 is not the only mechanism underlying the respiratory failure phenotype mediated with defective angiogenesis. MiR-126

downregulation in addition to global signaling deregulation finally lead to this phenotype. Many other molecules like those mediating TGF- β signaling, Ras/Raf/Erk and PI3K/Akt signaling could also mediate this phenotype. I recently found that loss of 14-3-3 ζ resulted in reduced HIF1- α , a well known oncogene that promotes angiogenesis by transcriptionally activate VEGF in multiple tissue types. It will be interesting to further study the how loss of 14-3-3 ζ lead to neonatal lethality. Measuring the HIF1- α expression in the embryo lungs may help us gain more function.

It will also be interesting to study whether miR-126 downregulation is playing a causal role in the lethality phenotype. I can either cross the 14-3-3 ζ knockout mouse to miR-126 transgenic mouse and test whether ectopically expressing miR-126 could rescue the phenotype.

MicroRNAs are able to target multiple mRNAs to regulate cellular processes. Many miR-126 targets have been reported to date. Spred-1 which is a suppressor of Ras/Raf/Erk signaling in response to VEGF stimulation is inhibited by miR-126 (76). VCAM1, which is a cell surface adhesion molecule, was upregulated in response to TNF- α stimulation when miR-126 is knocked down. Overexpression of VCAM1 resulted in more leukocyte adhesion to endothelial cells (91). This data matched my observation that more leukocytes are visible in the 14-3-3 ζ knockout embryo lungs especially around the blood vessels. In the future, it will be interesting to determine the expression level of the miR-126 targeting genes and test how important miR-126 is in this lethality phenotype.

3.3 Loss of 14-3-3 ζ inhibited mammary gland tumor formation and lung metastasis

3.3a Outbreeding rescues the lethality

The lethality hindered our study of 14-3-3 ζ role in adulthood diseases like cancer. As we found a proportion of homozygous mutant pups could survive the lethality in B6/129P2 hybrid genetic background, it is likely that outbreeding may circumvent the lethality phenotype. To test this, I outbred the 14-3-3 ζ knockout strain to CD-1. Approximately 25% of homozygous mutant pups were generated by mating heterozygous males and females after outbreeding (table 1), which indicated that the outbreeding rescued the neonatal lethality. The 14-3-3 ζ knockout mice could also breed without any obvious defect. At the same time, I also backcrossed the strain to FVB/N congenic background. The 14-3-3 ζ knockout mice under FVB/N genetic background were also viable and fertile.

3.3b Loss of 14-3-3 ζ did not significantly affect mammary gland development

In our initial attempt to study the role of 14-3-3 ζ in breast cancer, we first examined the mammary gland development in 14-3-3 ζ knockout mice.

Mammary glands were dissected from the mice at 4, 6, 8 and 12 weeks of age by biopsy. We performed whole mount staining of the mammary gland and found that the mammary gland parenchyma outgrowth was slightly delayed at 4 and 6 weeks of age in the knockout mice. The epithelial parenchyma in the wild type mammary gland exceeded the lymph node in contrast to that in the 14-3-3 ζ knockout mice barely touched the lymph node at 4 week of age. At the age of 8 weeks, the outgrowth of the duct was restored to that in the wild type mice (Figure 13). The 14-3-3 ζ knockout female mice could breed and nurse the pups, which also suggested that the 14-3-3 ζ knockout mammary glands were biologically functional.

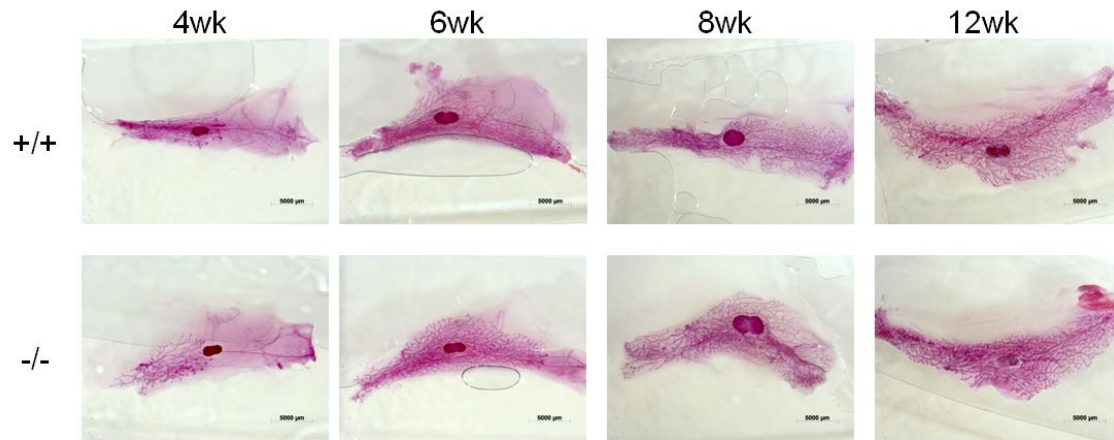


Figure 13. Loss of 14-3-3 ζ did not significantly affect mammary gland development. The fourth mammary glands from the left side of the mice were dissected at the time points of 4, 6, 8 and week of age as indicated. Whole mount staining was performed to determine the epithelial parenchyma outgrowth and branching. Scale bar indicates 5mm in length.

3.3c Loss of 14-3-3 ζ inhibited mammary gland tumor formation and metastasis induced by PyMT

To study the role of 14-3-3 ζ in breast cancer, we crossed the 14-3-3 ζ knockout mouse strain with MMTV promoter driven Polyoma middle T antigen (PyMT) transgenic strain which develops mammary gland tumor at an early age. The 14-3-3 ζ knockout mice had significantly longer latency of tumor onset. The mice were sacrificed when the tumor diameter reached 15 mm. The tumors were harvested for further study. Histological study of the tumor suggested that loss of 14-3-3 ζ did not affect the tumor subtype. The tumors from both wild type and 14-3-3 ζ knockout mice are invasive adenocarcinomas. The lungs were dissected to determine the number of lung metastases by visually counting the surface tumor nodules. The 14-3-3 ζ knockout mice had significantly lower number of lung metastases nodules (Figure 14).

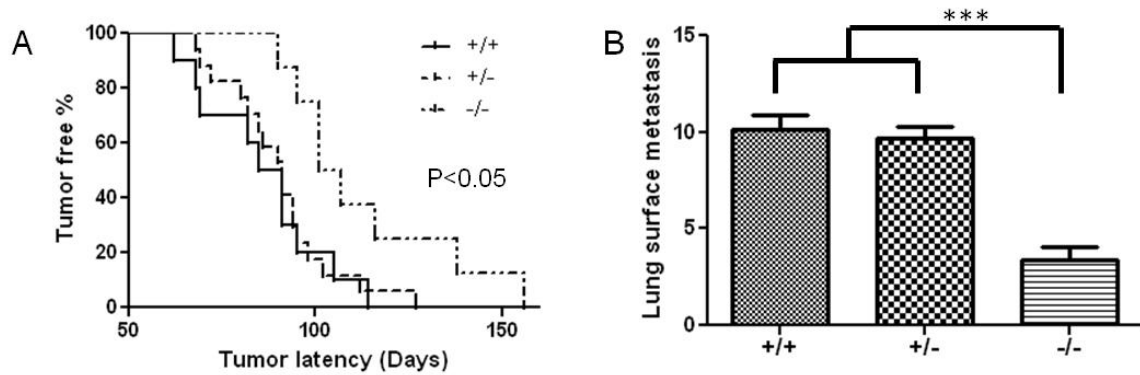


Figure 14. Loss of 14-3-3 ζ inhibited tumorigenesis and lung metastasis. A. 14-3-3 ζ homozygous mutant mice (-/-, n=8) had significantly longer tumor latency induced by PyMT compared to the wild type (+/+, n=10) and heterozygous mutant (+/-, n=17) counterparts. B. 14-3-3 ζ homozygous mutant mice had reduced lung metastasis as determined by surface tumor nodule number. *** indicates P value < 0.0001.

3.3d 14-3-3 ζ knockout tumors express lower 14-3-3 ζ level

Because the gene trap inactivates the expression of 14-3-3 ζ by utilizing the transcription splicing machinery, it is possible that the tumors in the knockout mice may arise from single cells that express comparable level of 14-3-3 ζ as that in wild type cells. We performed both western blot (Figure 17) and immunohistochemical staining on the tumors (Figure 15). We found that the tumors from the knockout mice expressed much lower level of 14-3-3 ζ compared to the tumors arising from the 14-3-3 ζ wild type mice. This suggested that the tumors from the knockout mice did not arise from cancer initiating cells expressing high level of 14-3-3 ζ . This data also suggested that knockdown of 14-3-3 ζ was not sufficient to completely inhibit PyMT oncogene induced tumor formation. To cure cancer expressing high level of 14-3-3 ζ need combination of other therapy regimen with 14-3-3 ζ target therapy.

3.3e Loss of 14-3-3 ζ affected multiple aspects in tumor biology by regulating multiple signaling pathways

Next I studied how loss of 14-3-3 ζ resulted in inhibited tumor formation and metastasis. By staining the tumor slides with proliferation marker Ki67, apoptosis marker TUNEL, and angiogenesis marker CD34, I found that the 14-3-3 ζ knockout tumors had reduced proliferation, increased apoptosis and reduced angiogenesis compared to their wild type counterparts (Figure 16).

To study the molecular mechanism underlying these biological changes in the 14-3-3 ζ knockout tumors, I started with a reverse phase protein array (RPPA) assay performed in the Functional Proteomics Reverse Phase Protein Array Facility at MD Anderson Cancer Center, which contained about 135 antibodies to determine what molecules were deregulated in 14-3-3 ζ knockout tumors. Two signaling pathways could be activated downstream of PyMT and those are the Ras/Raf/Erk and PI3K/Akt signaling pathways. , Both the signaling pathways were significantly inhibited in the knockout tumors as indicated by phospho-Raf-S388, phospho-Mek1-S217, phospho-Akt-T308 and phospho-Akt-S473 (Figure 17A). This finding was further validated by western blot. I found that phospho-Erk1/2-T202/Y204 and phospho-Akt-S473 was downregulated in the knockout tumors indicating the Ras/Raf/Erk and PI3K/Akt signaling pathways were inhibited in knockout tumors. I also found that the well known tumor suppressor p53 was upregulated in the knockout tumors. These data matched the previous reports that 14-3-3 ζ overexpression activated Akt and hence suppressed p53 via

phosphorylation-dependant activation of Mdm2 (69). Two molecules downstream of p53, the pro-apoptotic protein Bax which is transcriptionally activated by p53 was upregulated, whereas the pro-angiogenic protein VEGF transcriptionally suppressed by p53 was significantly downregulated. These data at least partially explained the reduced proliferation, angiogenesis and increased apoptosis as observed in knockout tumors (Figure 17B).

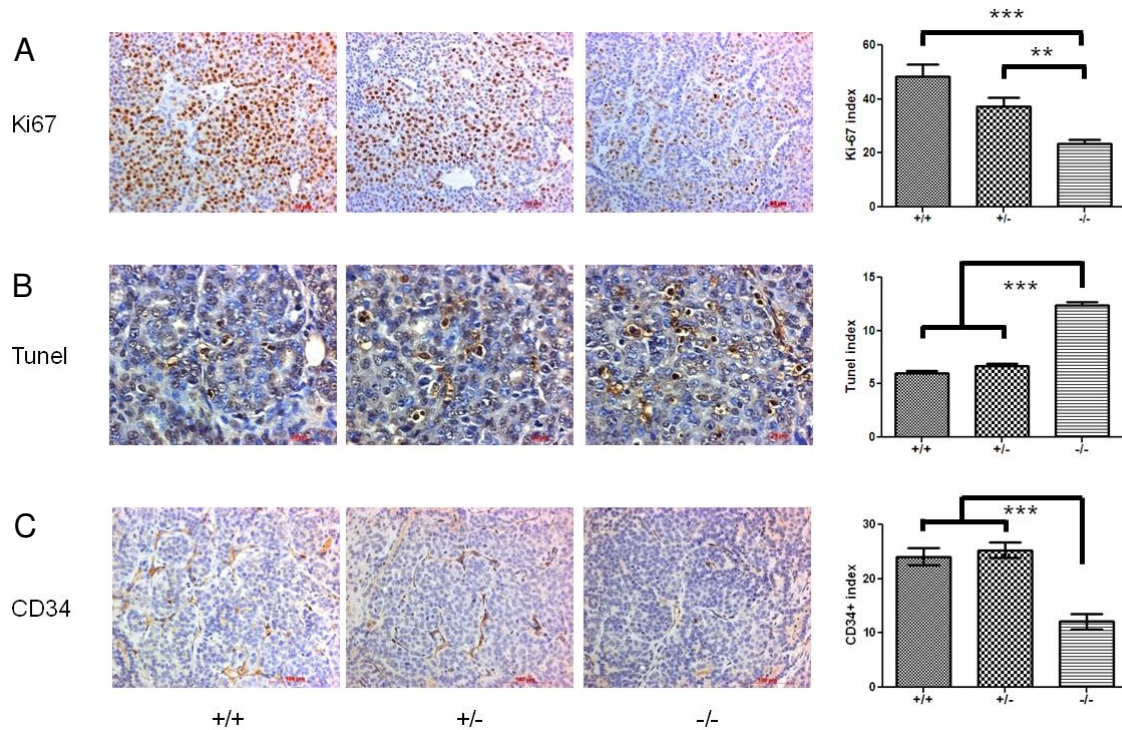


Figure 16. Loss of 14-3-3 ζ affected multiple aspects of cancer biology. A. Proliferation marker Ki67 was immunohistochemically staining in the tumor samples and quantified. Ki67 index indicates the percentage of Ki67 positive cells in 10 randomly selected fields. Scale bar indicates 50 μ m in length. B. Immunohistochemical staining of apoptosis marker Tunel and quantification. Tunel index indicates the Tunel positive cells in 10 randomly selected high power fields. Scale bar indicates 200 μ m in length. C. immunohistochemical staining of angiogenesis marker CD34 and quantification. CD34+ index indicates blood vessel numbers in 10 randomly selected fields. Scale bar indicates 100 μ m in length. Quantification data are presented as mean \pm standard error or the mean. ** indicates P-value <0.01, *** indicate P-value<0.0001.

JAVA tree. B. Western blot results confirmed that inactivation of Ras/Raf/Erk and PI3K/Akt in the 14-3-3 ζ knockout tumors as determined by p-Erk and p-Akt. Total Erk and Akt were blotted as control and β -actin was used as loading control. 14-3-3 ζ was blotted to confirm that 14-3-3 ζ expression was inhibited in the 14-3-3 ζ homozygous mutant tumors.

3.3f loss of 14-3-3 ζ inhibited tumorigenesis induced by Neu oncogene

Interestingly, we also found that PyMT expression level was also reduced 14-3-3 ζ knockout tumors (Figure 17). PyMT could bind to 14-3-3 ζ when phosphorylated on serine 257(23). S257 mutated PyMT inhibited salivary gland tumor formation compared to wild type viral antigen (92). To rule out the possibility that the inhibited tumor formation and metastasis was due to downregulated expression of PyMT mediated by loss of 14-3-3 ζ , we crossed the 14-3-3 ζ knockout strain with MMTV driven activated Neu (NDL 2-5) transgenic mouse strain. The 14-3-3 ζ knockout mice also exhibited delayed tumor onset induced by Neu (Figure 18), whereas the expression level of ErbB2 was not downregulated as determined by western blot (Figure 19). Immunohistochemical analysis confirmed that the 14-3-3 ζ knockout lead to reduced proliferation, angiogenesis and increased apoptosis (Figure 20). These data suggested that inhibition of tumor formation and metastasis is not due to downregulation of PyMT in the 14-3-3 ζ knockout mice but to the loss of 14-3-3 ζ mediated global signaling deregulation. So loss of 14-3-3 ζ could inhibit tumor formation in two different tumor prone mouse models.

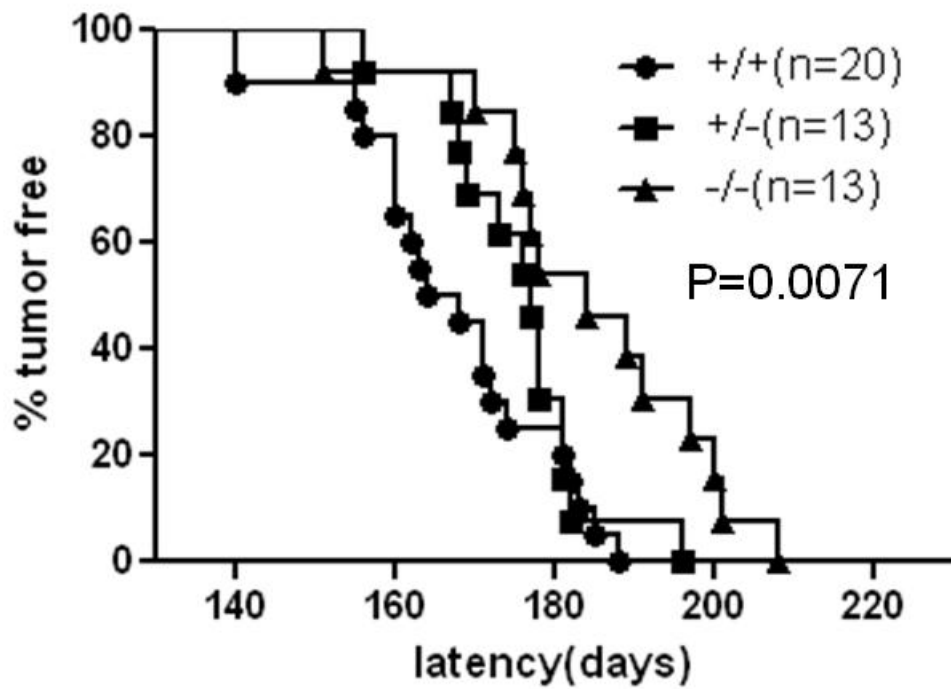


Figure 18. Loss of 14-3-3 ζ prolonged tumor latency induced neu oncogene. Kaplan-Meier curve study of the percentage of tumor free mice along with the age of the neu transgenic mice is diagramed. P-value is indicated as shown.

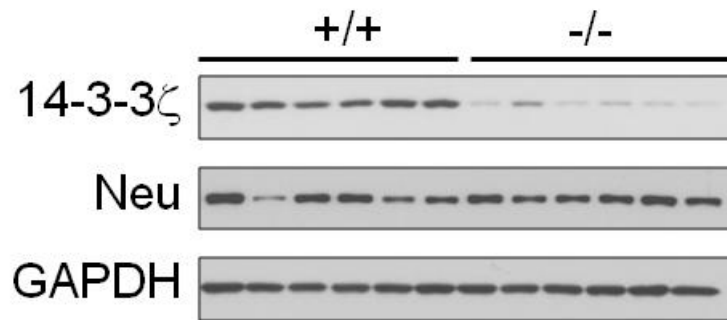


Figure 19. Neu oncogene expression was not affected in 14-3-3 ζ knockout tumors. Western blot of Neu in 14-3-3 ζ wild type and homozygous mutant tumors induced by neu oncogene. GAPDH was used as loading control.

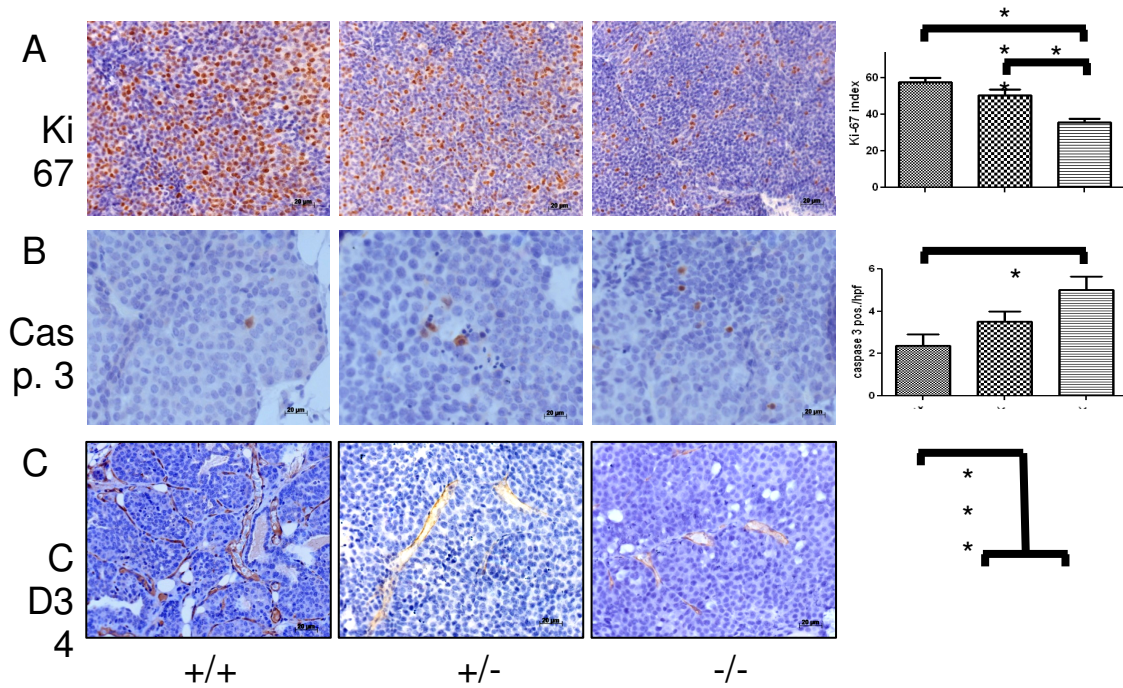


Figure 20. Loss of 14-3-3 ζ affects tumor biology in Neu oncogene induced tumors. A. Immunohistochemical staining of proliferation marker Ki67 and quantification. Ki67 index was calculated as percentage of Ki67 positive cells in 10 randomly selected fields. B. Immunohistochemical staining of apoptosis marker caspase 3 and quantification as average caspase 3 positive cell numbers every high power field (hpf) from 10 randomly selected fields. C. Immunohistochemical staining of angiogenesis marker CD34 and quantification. CD34+ index indicates the average blood vessel number per hpf from 10 randomly selected fields. Scale bar indicates 200um in length. Quantification data presented as mean \pm standard error of the mean. * indicates P-value<0.05, ** indicates P-value<0.01 and *** indicates P-value<0.001.

3.3g miR-126 is downregulated in 14-3-3 ζ knockout tumors

I previously found that microRNA-126 was along with defective angiogenesis downregulated in 14-3-3 ζ knockout lung tissues. Angiogenesis was also reduced in 14-3-3 ζ knockout tumors. In my initial test whether miR-126 was also an important mediator of defective angiogenesis induced by loss of 14-3-3 ζ in tumors, I used quantitative real-time RT-PCR to measure miR-126 expression level in the tumor samples and found that miR-126 was significantly downregulated in 14-3-3 ζ knockout tumors (Figure 21).

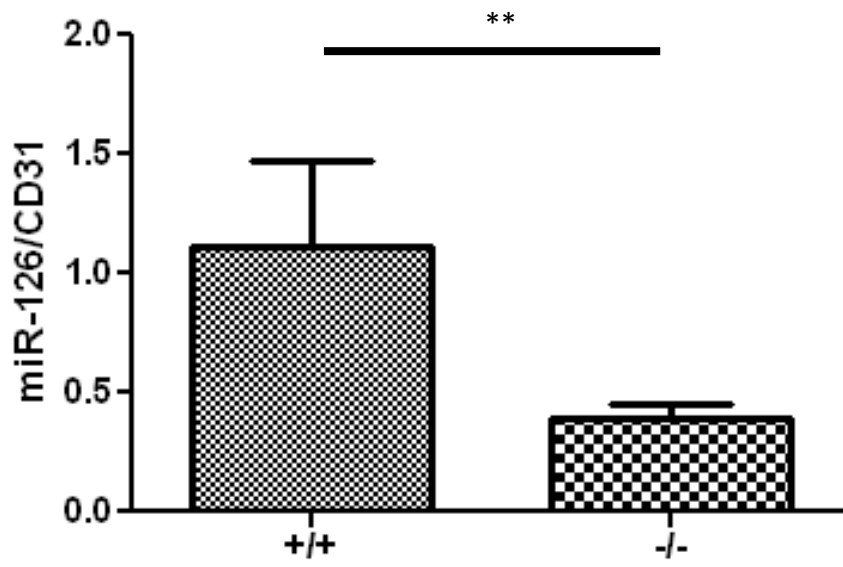


Figure 21. MicroRNA-126 was downregulated in 14-3-3 ζ knockout tumors. Total RNA was extracted from wild type and 14-3-3 ζ knockout tumor tissues induced by PyMT. qRT-PCR of miR-126 was performed and normalized to PECAM1/CD31. Fold change of miR-126/CD31 ratio is presented as mean \pm standard error of the mean. ** indicates P-value < 0.01.

3.3h miR-126 regulates angiogenesis downstream of 14-3-3 ζ

To further test whether miR-126 was one of the key players in the angiogenesis defect mediated by loss of 14-3-3 ζ . First of all, I transfected the mouse endothelial cell line with scramble or 14-3-3 ζ shRNA and found that knocking down 14-3-3 ζ significantly inhibited the angiogenic capability of the mouse endothelial cells as determined by transwell migration assay and tube formation assay (Figure 22). This *in vitro* result supported the *in vivo* finding that 14-3-3 ζ was critical in angiogenesis both in embryo lungs and tumors. When I transfected the 14-3-3 ζ knockout down cells with pre-miR-126, the angiogenic capability was restored (Figure 22). These data suggested that miR-126 was a key regulator of angiogenesis downstream of 14-3-3 ζ .

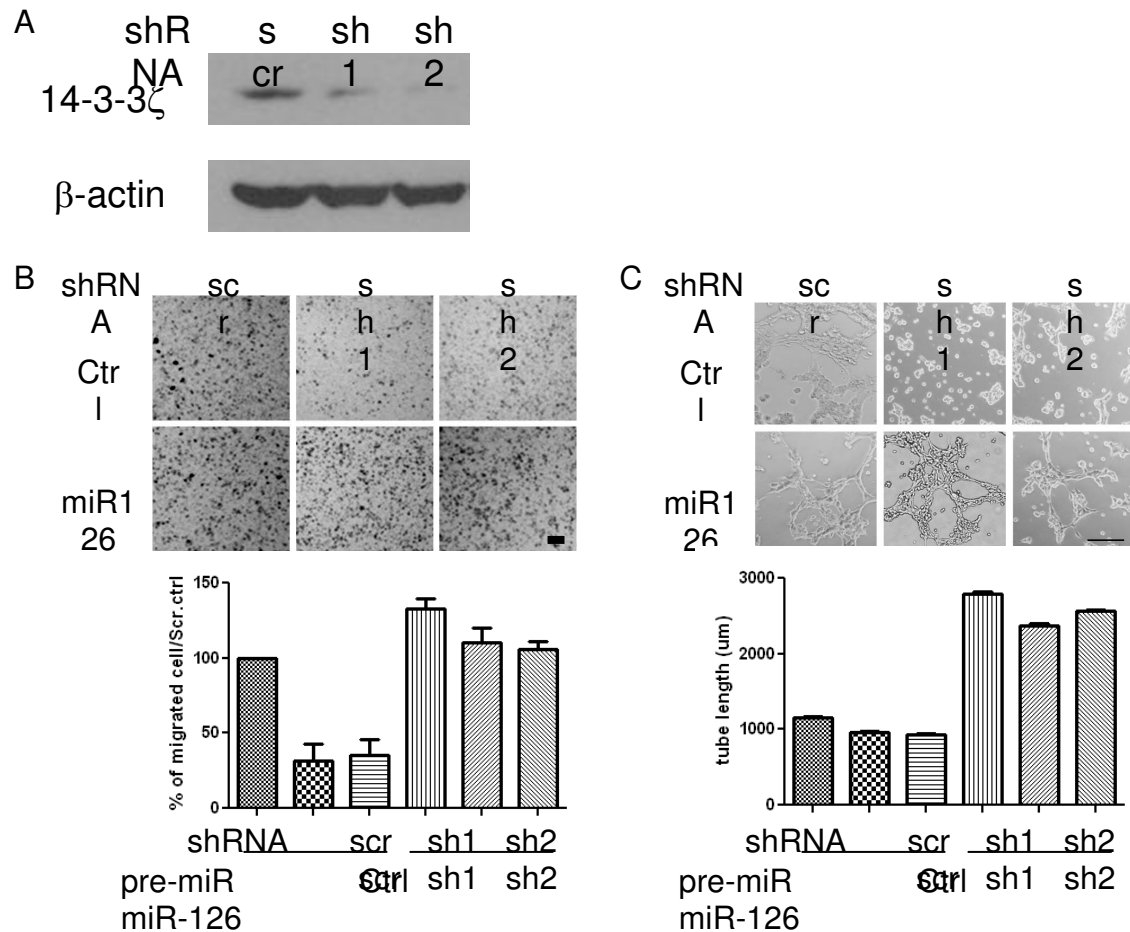


Figure 22. microRNA-126 regulates angiogenesis downstream of 14-3-3 ζ . A. Mouse endothelial cells were transfected with scramble or 2 independent 14-3-3 ζ shRNAs. 14-3-3 ζ knockdown efficiency was determined by western blot. β -actin was used as loading control. B. Image of the transwell migration assay and quantification. Cells transfected with scramble or 14-3-3 ζ shRNA in combination with control pre-microRNA or pre-miR-126 were tested for the migration capability. Migrated cells were stained with crystal violet, imaged and quantified with ImageJ. Data presented as mean \pm standard error of the mean. C. Image of the tube formation assay and quantification. The cells were seeded on matrigel and cultured in incubator for 4-12 hours and imaged. Tube formation capability

was determined by the average length of the tube structure formed every high power field. Assays were repeated 3 times. Data presented as mean \pm standard error of the mean.

3.3i Discussion

14-3-3 ζ has been considered a potential oncogene and therapy target. Here we found that loss of 14-3-3 ζ significantly inhibited tumorigenesis, progression and lung metastasis in two different tumor prone mouse models.

Hundreds of proteins have been reported to form complexes with 14-3-3 ζ . It was not a surprising to see in the RPPA analysis that many genes expression are differential between the wild type and 14-3-3 ζ knockout tumors. With the global signaling deregulation, I can easily explain the tumor biology change such as reduced proliferation, increased apoptosis and reduced angiogenesis in the 14-3-3 ζ knockout tumors. This inhibited tumorigenesis and lung metastasis suggested to me that 14-3-3 ζ can be a potential therapy target. Though knocking down of 14-3-3 ζ alone could not completely inhibit tumor formation or cure tumor, one can try treating the mice with chemo- or radioactive therapeutic regimens and test the potential of combinational therapy. As in clinic many targeted therapies are used in combination with chemotherapy, it is possible that combinational therapy could cure the tumor.

MicroRNA-126 has been shown to be downregulated in 14-3-3 ζ knockout embryo lungs. Here miR-126 is also downregulated along with reduced angiogenesis in 14-3-3 ζ knockout tumors suggesting miR-126 regulation by 14-3-3 ζ is a conserved signaling both in lung development and tumor progression. MiR-126 role in cancer remains controversial. Some published papers argue that miR-126 functions as a tumor suppressor in breast cancer (84, 93, 94). It was

hypothesized that downregulation of miR-126 could result in leaky blood vessel and thus enhancing metastasis. However, these studies were performed using epithelial cell lines or the whole tumor in which epithelial cells were the major compartment, whereas miR-126 expression was restricted in endothelial cells. So it would be reasonable to normalize the miR-126 expression level to endothelial specific housekeeping gene. As I mentioned, I used PECAM1 as control in this study. How miR-126 functions in cancer remains to be further studied.

3.4 14-3-3 ζ knockout mice are growth retarded

3.4a 14-3-3 ζ knockout mice are smaller than their littermates

Interestingly, except the inhibited tumor formation and progression, I also observed that the 14-3-3 ζ knockout mice are smaller than their wild type and heterozygous littermates after outbreeding (Figure 23). They weigh less than their wild type counterparts since 2 week of age. The difference got most significant at 3 and 4 week of age. Then the knockout mice could catch up to some extent later (Figure 23). Because the time matched the puberty onset in mice, this data suggested that the 14-3-3 ζ knockout mice seemed to be smaller and have late onset of puberty and are growth retarded.

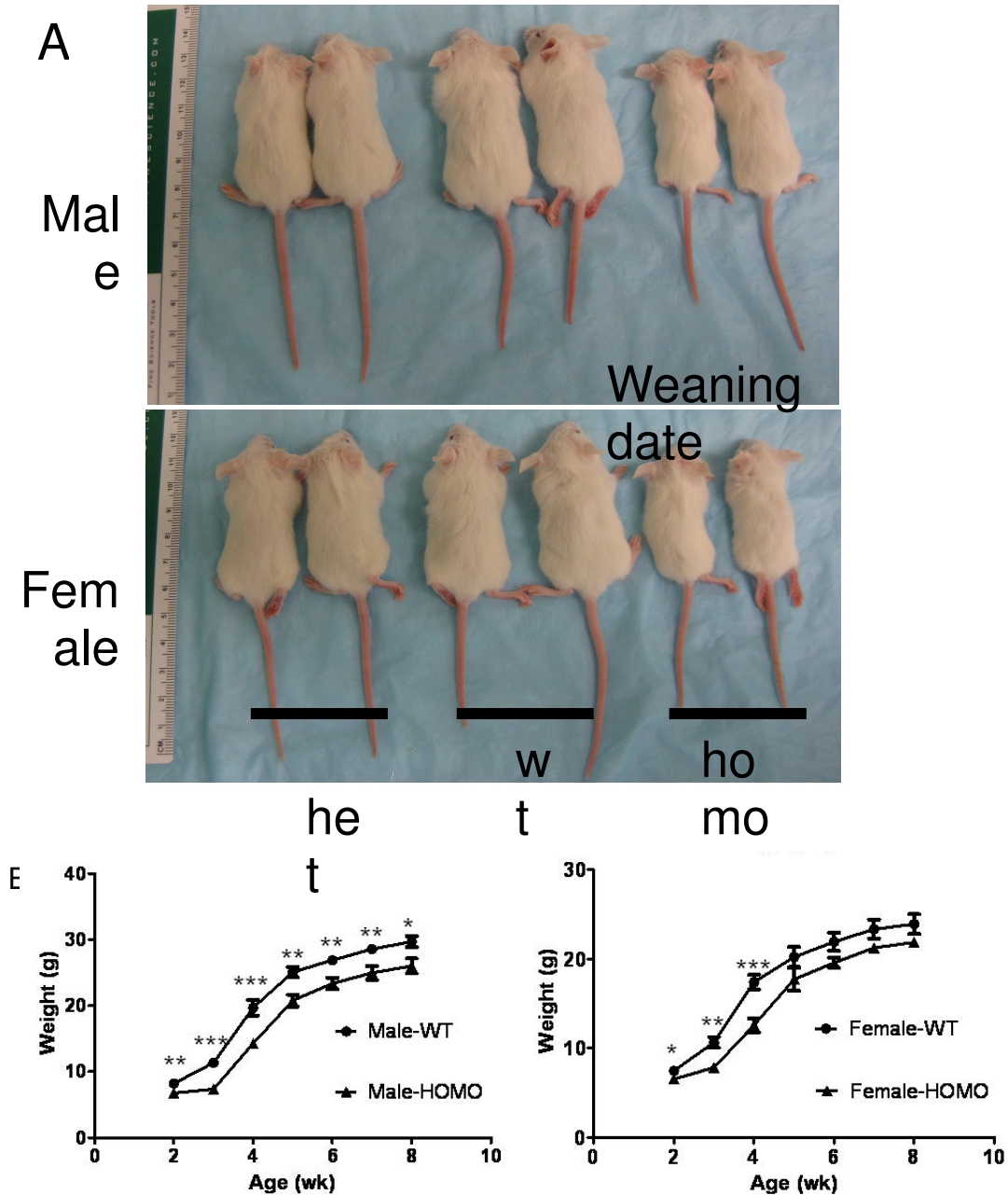


Figure 23. 14-3-3 ζ knockout mice are growth retarded. A. Image of the 14-3-3 ζ wild type (wt), heterozygous (het) and homozygous mutant (homo) mice on the weaning date which is 3 week of age. Top panel image was taken on male mice in one litter and bottom panel was taken on female mice from one litter. B. Mouse weight along with the age. Weigh data gram (g) were obtained from 2 to

8 week (wk) of age from wild type and homozygous mutant mice presented as mean \pm standard error of the mean. * indicates P-value<0.05, ** indicates P-value<0.01 and *** indicates P-value<0.0001.

3.4b 14-3-3 ζ knockout mice had reduced growth hormone but increased IGF-1 in circulation

As the most significant difference in weight between wild type and the knockout mice was observed at the age around 3-4 weeks which matched the puberty onset in mice, it suggested that 14-3-3 ζ had impact on puberty onset in mouse. Growth hormone and insulin-like growth factors are well documented to regulate pubertal growth (95-98). I measured circulating growth hormone and IGF-1 to start with. Interestingly, compared to the reduced growth hormone level in the knockout mice circulation as I expected, the serum IGF-1 level was significantly increased in the knockout mice blood (Figure 24).

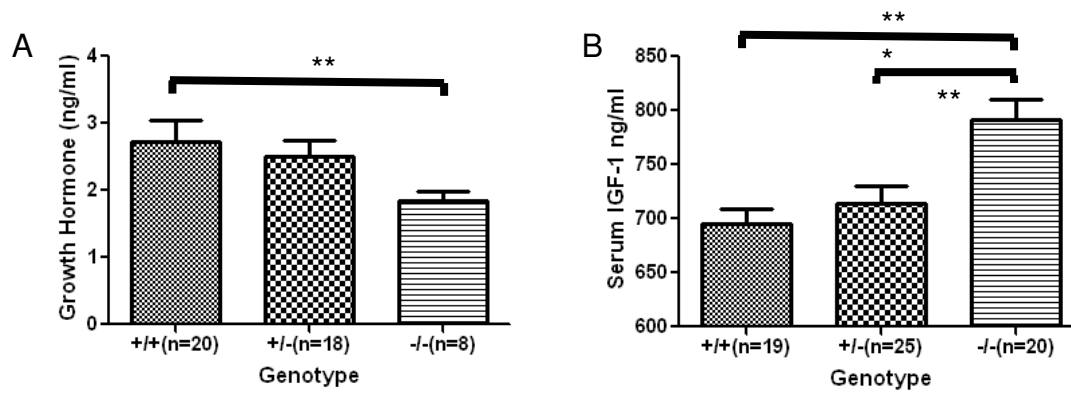


Figure 24. Loss of 14-3-3 ζ lead to aberrance in growth related hormonal expression. A. Serum samples were drawn from 4 week old mice tail vein. Growth hormone level was measure using ELISA following standard protocol. B. Active IGF-1 level was measured using RIA kit following the product instruction. Sample size of each group was indicated in the figure. ** indicates P-value<0.01 and *** indicates P-value< 0.0001.

3.4c 14-3-3 ζ knockout mice had aberrant glucose homeostasis

As I observed the increased IGF-1 in the 14-3-3 ζ knockout mouse circulation in contrast to our expectation, and IGF-1 and its receptors play critical role in regulating growth and glucose homeostasis, I tested whether there was any aberrance in glucose homeostasis in the 14-3-3 ζ knockout mice.

Interestingly, I found that the blood glucose level in the knockout mice was significantly lower than that of the wild type mice (Figure 25). As IGF-1 promotes glucose uptake and regulates glucose homeostasis (99, 100), this data matched the observation of increased IGF-1 level in the 14-3-3 ζ knockout serum.

However, interestingly, loss of 14-3-3 ζ inhibited Akt activation observed in multiple studies including the tumorigenesis study induced by PyMT as previously described in this dissertation. Akt promotes glucose uptake by regulating multiple signaling pathways (101). Next I did glucose tolerance assay to better understand how 14-3-3 ζ impacts glucose homeostasis. Remarkably, I found that though the basal blood glucose level was lower in the 14-3-3 ζ knockout mice after 16 hour fasting, after glucose challenge, the glucose clearance from the blood was much slower in the knockout mice compared to the wild type counterparts. This data suggested that the glucose uptake was inhibited in the 14-3-3 ζ knockout mouse tissues. To test this, I injected the mice with a fluorescent glucose homolog, 2-NBDG into the mice via i.v., harvested the brain and liver tissues which are the tissues uptake majority of glucose from circulation and measured the glucose uptake level indicated by 2-NBDG fluorescence intensity. I found the 2-NBDG level in the 14-3-3 ζ knockout mice

brain and liver tissues was much lower than that in the wild type tissue (Figure 26).

Based on these data, I conclude that 14-3-3 ζ affected glucose homeostasis.

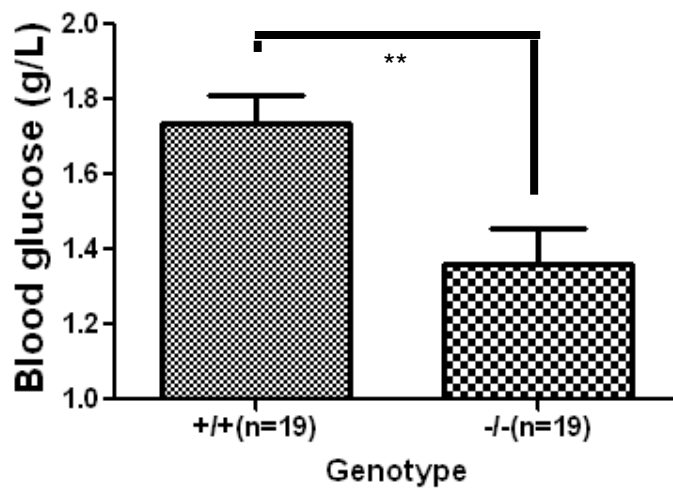


Figure 25. Loss of resulted in lower blood glucose. A drop of blood was drawn from mouse tail snip ad libitum. Blood glucose was measure using Roche AccuChek blood glucose meter. Sample size was indicated as shown. ** indicates P-value<0.01.

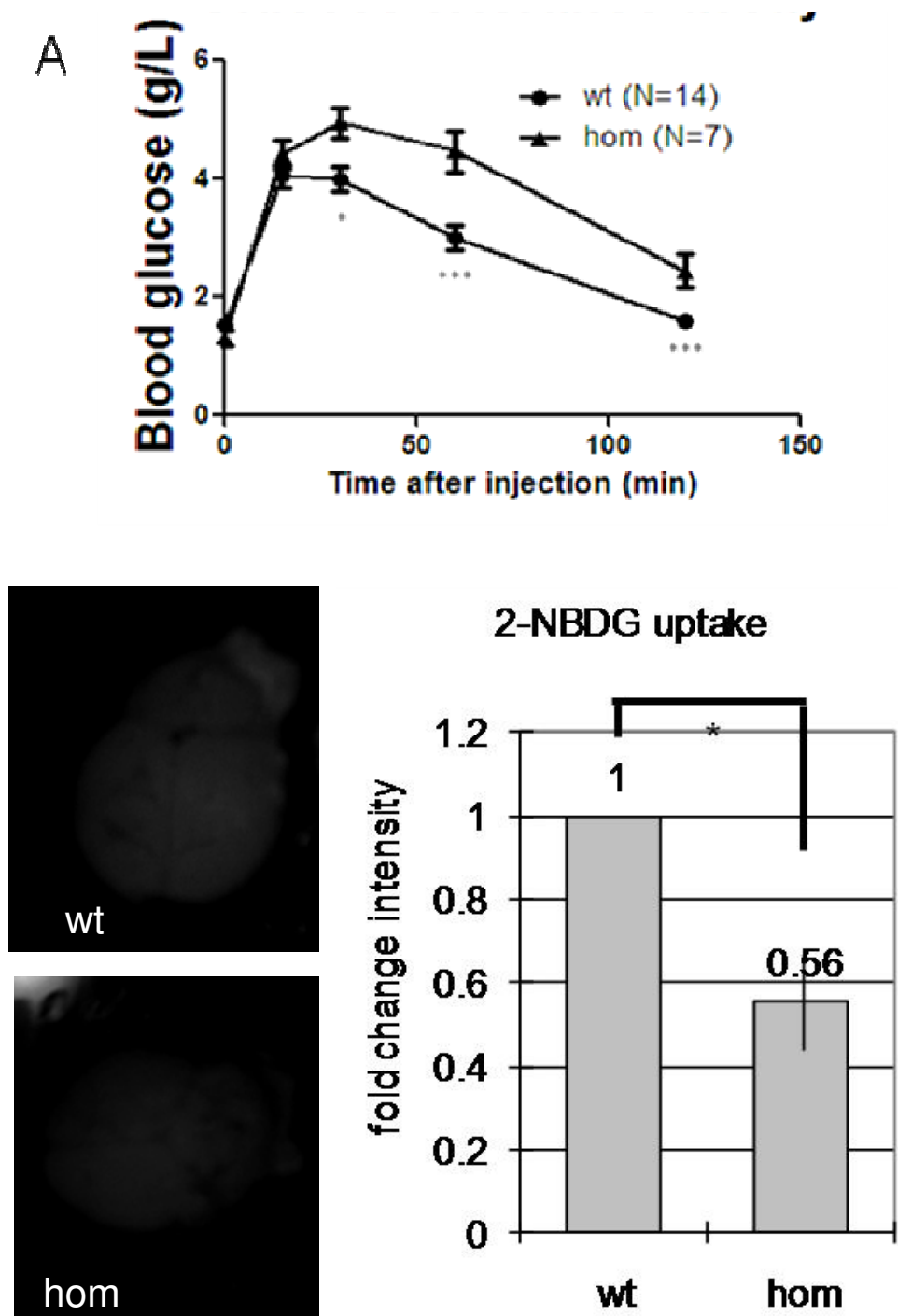


Figure 26. 14-3-3 ζ regulates glucose uptake. A. 14-3-3 ζ null mice had impaired glucose tolerance. Age matched 14-3-3 ζ wild type (wt) and knockout (homo) mice were fasted 16 hours. 3g/kg weigh glucose was injected intraperitoneally.

Blood glucose was measured using blood retrieved from the tail snips at the time points indicated in the figure. * and *** indicated that the blood glucose levels were statistically significantly different between the groups. (*, $P < 0.05$; ***, $P < 0.001$). B. Representative images of 2-NBDG fluorescent signal in 14-3-3 ζ wild type and 14-3-3 ζ knockout mouse brain visualized by the Maestro system. Fold change of 2-NBDG signal intensity quantified by Image J software. Data presented as mean \pm standard error of the mean. * indicates statistical P -value < 0.05 .

3.4d molecular mechanism underlying the defective glucose homeostasis

Then I wondered what was the molecular mechanism mediating the reduced glucose uptake. HIF1- α and IGF1R caught my attention. HIF1- α , hypoxia induced factor 1 alpha, is a well known transcription factor that regulates glucose homeostasis, angiogenesis and cell survival by transcriptionally activate PGK1, LDH1, Glut1 and other hypoxia responsive genes like VEGF (102, 103). 14-3-3 ζ overexpression activates Akt (69), which is also involved in reprogramming of metabolic genes. Additionally, activation of mTOR, downstream of Akt, could lead to activation of HIF1- α that could drive the major cancer metabolic changes (104). IGF1R activates PI3K/Akt signaling pathway and can regulates glucose homeostasis (105). Loss of IGF1R resulted in neonatal lethality due to respiratory failure and severe dwarfism (106). I measured the expression level of HIF1- α in mouse mammary gland and IGF1R in mouse embryonic fibroblast (MEF) cells. I found that HIF1- α and IGF1R expression level was significantly downregulated in 14-3-3 ζ knockouts (Figure 27). So HIF1- α and IGF1R can be regulated by 14-3-3 ζ to maintain glucose homeostasis.

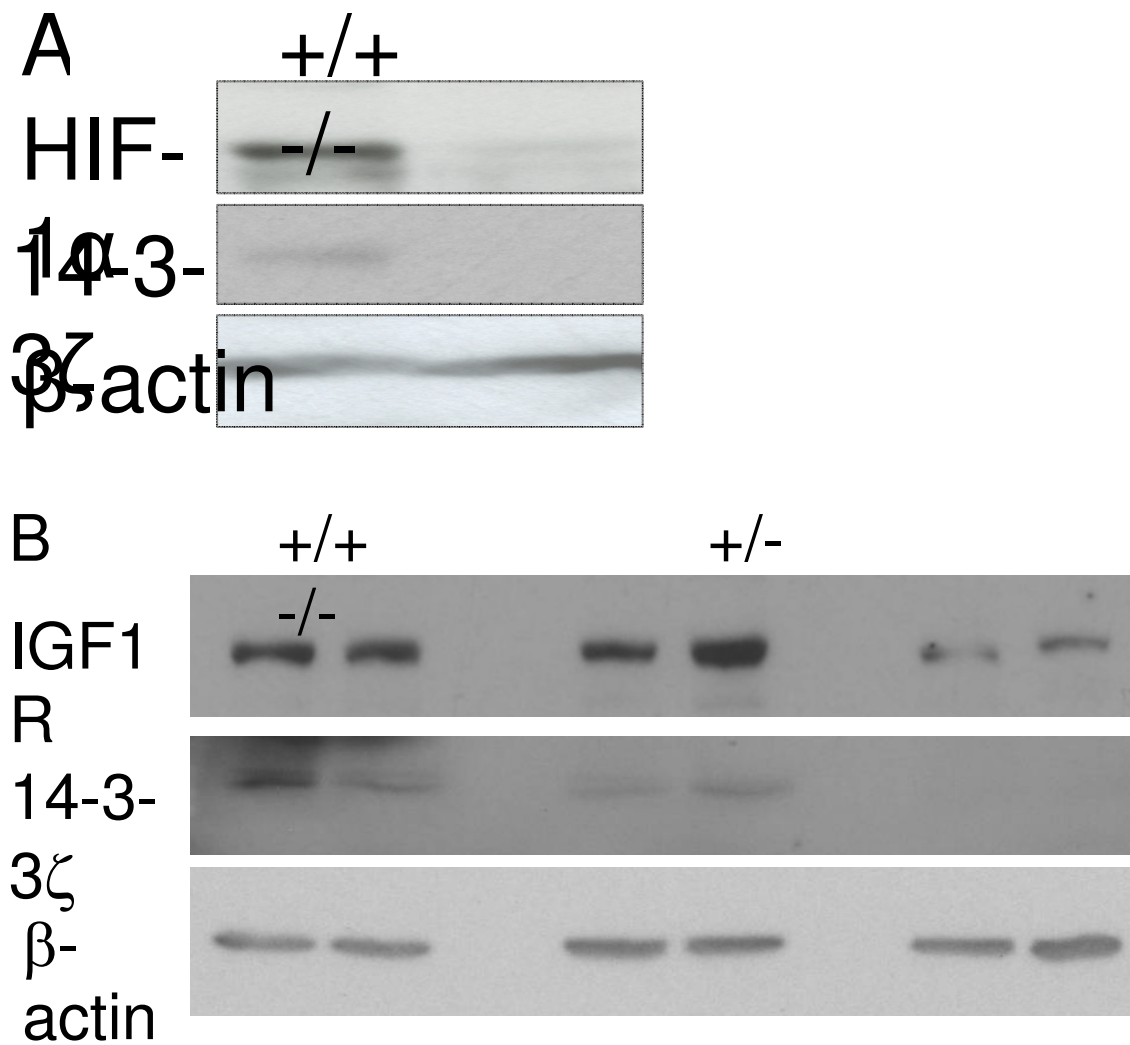


Figure 27. 14-3-3 ζ regulates HIF1- α and IGF1R. A. Loss of 14-3-3 ζ downregulated HIF1- α . Protein lysates extracted from mammary glands of wild type (+/+) and knockout (-/-) mice. B. Loss of 14-3-3 ζ downregulated IGF1R. Protein lysate extracted from immortalized mouse embryonic fibroblast (MEF) cells generated from wild type (+/+), heterozygous (+/-) and 14-3-3 ζ homozygous knockout (-/-) mouse embryos.

3.4e Discussion

Growth hormone/Igf-1 axis signaling has been reported to regulated mammary gland development (107), animal stature(106) and glucose homeostasis (108). Growth hormone is secreted by the pituitary into the circulation and promotes IGF-1 expression in peripheral tissues, mainly in liver to promote cell growth (109).

It is interesting that I found reduced cellular IGF1R and increased IGF-1 in circulation. This data indicated that reduced receptor level rendered the tissues insensitive to the IGF-1 ligand. To maintain homeostasis, the tissues may express more ligand to keep the balance. This is typically true in growth retarded patients resistant to IGF-1 (110-113). This phenomenon is similar to type II diabetes in which the tissues are resistant to insulin. Pancreas β -cells had to express more insulin to keep normal glucose level after feeding. This will result in high blood glucose level along with high insulin. When the IGF-1 level was higher in 14-3-3 ζ knockout mouse blood, a feedback signaling would make the pituitary express less growth hormone. This may explain the phenomenon such as delayed puberty onset and reduced blood glucose level I observed in the animal.

Insulin, compared to IGF-1, is more efficient to promote glucose uptake but tightly regulated by blood glucose level, whereas IGF-1 regulates glucose homeostasis in a more consistent manner. IGF1R deletion also rendered the β -islet cells secret lower insulin (114, 115). As to that the 14-3-3 ζ knockout mice

also displayed better glucose tolerance, it would be interesting to further measure the insulin level and β -cell function in the knockout mouse and study the differential role of insulin and IGF-1 in regulating glucose homeostasis.

GH/IGF-1 axis is also involved in puberty onset and mammary gland development. I also observed that the mammary gland development is slightly delayed in the 14-3-3 ζ knockout mice matching the delayed puberty phenotype. Meanwhile, the IGF1R also plays important role in breast cancer formation and therapy resistance (116, 117). It is expected that IGF1R plays important role not only in the delayed puberty, mammary gland development and aberrant glucose homeostasis, but tumorigenesis and progression inhibition. Further study of how 14-3-3 ζ regulates IGF1R may provide insight of breast cancer formation progression and resistance to therapeutic regimens.

Recent studies suggest that metabolism plays important role in cancer (118-120). Our data strongly suggested that 14-3-3 ζ plays important role in regulating metabolism likely through HIF1- α and IGF1R. Both of these genes regulate cancer progression (121, 122). More interestingly both the genes regulate angiogenesis (123-126). Many studies have suggested the important role of 14-3-3 ζ in cancer. 14-3-3 ζ can be a new bridge linking cancer and metabolism and provide new insight in cancer therapy.

I found that miR-126 was downregulated in 14-3-3 ζ knockout embryos lungs and tumors. It is also reported that miR-126 was reduced in type II diabetes patients' sera (79). Its role in diabetes is not clear yet. The 14-3-

3ζ knockout mice may be resistant to insulin as indicated by better glucose tolerance. It will be interesting to further investigate whether miR-126 is playing some role mediating the energy deregulation caused by loss of 14-3-3ζ. Ptpn9 which is a target of miR-126 is a phosphatase of EGFR and ErbB2 (127, 128). It has been reported to be involved in diabetes and cancer (129, 130). Currently I am studying its role in both cancer and glucose homeostasis.

3.5 Other phenotypes in 14-3-3 ζ knockout mouse

The 14-3-3 ζ knockout mice have other phenotypes to be further characterized. For example, the 14-3-3 ζ knockout mouse did not spread out the rear limbs like the wild type mouse when lifted up via the tail, which suggested neuronal degeneration phenotype (Figure 28). As 14-3-3 ζ has been reported to be involved in many human diseases as described in the introduction part of the thesis, it would be interesting to further study the function of 14-3-3 ζ in those specific tissues.

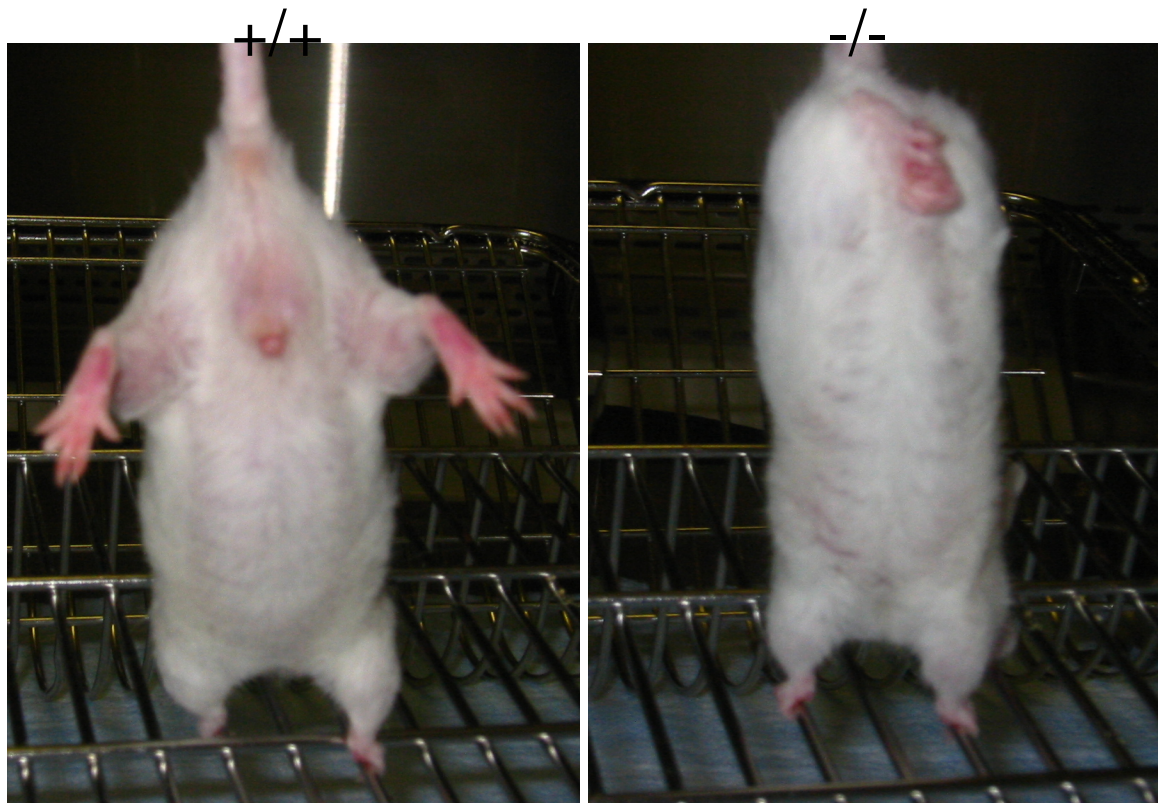


Figure 28. 14-3-3 ζ knockout mice display phenotype indicative of neuronal degeneration. The wild type mouse (left panel) spread the rear limbs outward when lifted up. The knockout mouse (right panel) clasped.

Chapter 4 Summary and Future Direction

In my thesis work, I generated a 14-3-3 ζ hypomorphic mutant mouse strain. This animal model displayed multiple phenotypes under different genetic background such as neonatal lethality, delayed puberty, tumorigenesis inhibition and aberrant glucose homeostasis. I studied the function of 14-3-3 ζ using this model and gained initial insight about the 14-3-3 ζ role and the molecular mechanisms mediating these *in vivo*.

I found different phenotypes in different genetic background. Loss of 14-3-3 ζ resulted in neonatal lethality in C57Bl/6 genetic background due to respiratory failure. Loss of 14-3-3 ζ inhibited tumorigenesis and progression in CD-1 and FVB/N genetic background. 14-3-3 ζ mice are smaller and have delayed puberty onset in CD-1 strain. More phenotypes are to be characterized to study 14-3-3 ζ *in vivo* function.

Using this model, we can better understand the role of 14-3-3 ζ in human diseases like cancer. In the future, we may develop new target therapy related to 14-3-3 ζ to treat and benefit patients in clinic.

This strain is a whole body knockout mouse model. Now we know tissue microenvironment is critical for cellular function. A mouse model in which we can conditionally or inducibly manipulate the 14-3-3 ζ could help us better understand the role of 14-3-3 ζ *in vivo*. I designed a tetracycline inducible 14-3-3 ζ transgenic mouse strategy and this transgenic mouse strain has been

available in the lab now. We can generate more in depth insight of 14-3-3 ζ function using this model in the near future.

Reference

1. Lakhani, S. R. 1999. The transition from hyperplasia to invasive carcinoma of the breast. *The Journal of pathology* 187:272-278.
2. Polyak, K. 2001. On the birth of breast cancer. *Biochimica et biophysica acta* 1552:1-13.
3. Vargo-Gogola, T., and J. M. Rosen. 2007. Modelling breast cancer: one size does not fit all. *Nat Rev Cancer* 7:659-672.
4. Dougherty, M. K., and D. K. Morrison. 2004. Unlocking the code of 14-3-3. *J Cell Sci* 117:1875-1884.
5. Moore, J. C. 1967. Human Nervous System - Noback, Cr. *American Journal of Occupational Therapy* 21:399-399.
6. Boston, P. F., P. Jackson, and R. J. Thompson. 1982. Human 14-3-3 protein: radioimmunoassay, tissue distribution, and cerebrospinal fluid levels in patients with neurological disorders. *J Neurochem* 38:1475-1482.
7. Aitken, A., D. Jones, Y. Soneji, and S. Howell. 1995. 14-3-3 proteins: biological function and domain structure. *Biochem Soc Trans* 23:605-611.
8. Fu, H., R. R. Subramanian, and S. C. Masters. 2000. 14-3-3 proteins: structure, function, and regulation. *Annu Rev Pharmacol Toxicol* 40:617-647.

9. Ichimura, T., T. Isobe, T. Okuyama, T. Yamauchi, and H. Fujisawa. 1987. Brain 14-3-3 protein is an activator protein that activates tryptophan 5-monooxygenase and tyrosine 3-monooxygenase in the presence of Ca^{2+} , calmodulin-dependent protein kinase II. *FEBS Lett* 219:79-82.
10. Craparo, A., R. Freund, and T. A. Gustafson. 1997. 14-3-3 (epsilon) interacts with the insulin-like growth factor I receptor and insulin receptor substrate I in a phosphoserine-dependent manner. *J Biol Chem* 272:11663-11669.
11. Furlanetto, R. W., B. R. Dey, W. Lopaczynski, and S. P. Nissley. 1997. 14-3-3 proteins interact with the insulin-like growth factor receptor but not the insulin receptor. *Biochem J* 327 (Pt 3):765-771.
12. Fantl, W. J., A. J. Muslin, A. Kikuchi, J. A. Martin, A. M. MacNicol, R. W. Gross, and L. T. Williams. 1994. Activation of Raf-1 by 14-3-3 proteins. *Nature* 371:612-614.
13. Fu, H., K. Xia, D. C. Pallas, C. Cui, K. Conroy, R. P. Narsimhan, H. Mamon, R. J. Collier, and T. M. Roberts. 1994. Interaction of the protein kinase Raf-1 with 14-3-3 proteins. *Science* 266:126-129.
14. Irie, K., Y. Gotoh, B. M. Yashar, B. Errede, E. Nishida, and K. Matsumoto. 1994. Stimulatory effects of yeast and mammalian 14-3-3 proteins on the Raf protein kinase. *Science* 265:1716-1719.

15. Freed, E., M. Symons, S. G. Macdonald, F. McCormick, and R. Ruggieri. 1994. Binding of 14-3-3 proteins to the protein kinase Raf and effects on its activation. *Science* 265:1713-1716.
16. Luo, Z. J., X. F. Zhang, U. Rapp, and J. Avruch. 1995. Identification of the 14.3.3 zeta domains important for self-association and Raf binding. *J Biol Chem* 270:23681-23687.
17. Li, S., P. Janosch, M. Tanji, G. C. Rosenfeld, J. C. Waymire, H. Mischak, W. Kolch, and J. M. Sedivy. 1995. Regulation of Raf-1 kinase activity by the 14-3-3 family of proteins. *EMBO J* 14:685-696.
18. Reuther, G. W., H. Fu, L. D. Cripe, R. J. Collier, and A. M. Pendergast. 1994. Association of the protein kinases c-Bcr and Bcr-Abl with proteins of the 14-3-3 family. *Science* 266:129-133.
19. Ogihara, T., T. Isobe, T. Ichimura, M. Taoka, M. Funaki, H. Sakoda, Y. Onishi, K. Inukai, M. Anai, Y. Fukushima, M. Kikuchi, Y. Yazaki, Y. Oka, and T. Asano. 1997. 14-3-3 protein binds to insulin receptor substrate-1, one of the binding sites of which is in the phosphotyrosine binding domain. *J Biol Chem* 272:25267-25274.
20. Garcia-Guzman, M., F. Dolfi, M. Russello, and K. Vuori. 1999. Cell adhesion regulates the interaction between the docking protein p130(Cas) and the 14-3-3 proteins. *J Biol Chem* 274:5762-5768.

21. Conklin, D. S., K. Galaktionov, and D. Beach. 1995. 14-3-3 proteins associate with cdc25 phosphatases. *Proc Natl Acad Sci U S A* 92:7892-7896.
22. Zha, J., H. Harada, E. Yang, J. Jockel, and S. J. Korsmeyer. 1996. Serine phosphorylation of death agonist BAD in response to survival factor results in binding to 14-3-3 not BCL-X(L). *Cell* 87:619-628.
23. Pallas, D. C., H. Fu, L. C. Haehnel, W. Weller, R. J. Collier, and T. M. Roberts. 1994. Association of polyomavirus middle tumor antigen with 14-3-3 proteins. *Science* 265:535-537.
24. Tzivion, G., V. S. Gupta, L. Kaplun, and V. Balan. 2006. 14-3-3 proteins as potential oncogenes. *Semin Cancer Biol* 16:203-213.
25. Muslin, A. J., J. W. Tanner, P. M. Allen, and A. S. Shaw. 1996. Interaction of 14-3-3 with signaling proteins is mediated by the recognition of phosphoserine. *Cell* 84:889-897.
26. Yaffe, M. B., and A. E. Elia. 2001. Phosphoserine/threonine-binding domains. *Curr Opin Cell Biol* 13:131-138.
27. Yaffe, M. B., K. Rittinger, S. Volinia, P. R. Caron, A. Aitken, H. Leffers, S. J. Gamblin, S. J. Smerdon, and L. C. Cantley. 1997. The structural basis for 14-3-3:phosphopeptide binding specificity. *Cell* 91:961-971.

28. Rittinger, K., J. Budman, J. Xu, S. Volinia, L. C. Cantley, S. J. Smerdon, S. J. Gamblin, and M. B. Yaffe. 1999. Structural analysis of 14-3-3 phosphopeptide complexes identifies a dual role for the nuclear export signal of 14-3-3 in ligand binding. *Mol Cell* 4:153-166.
29. Liu, D., J. Bienkowska, C. Petosa, R. J. Collier, H. Fu, and R. Liddington. 1995. Crystal structure of the zeta isoform of the 14-3-3 protein. *Nature* 376:191-194.
30. Xiao, B., S. J. Smerdon, D. H. Jones, G. G. Dodson, Y. Soneji, A. Aitken, and S. J. Gamblin. 1995. Structure of a 14-3-3 protein and implications for coordination of multiple signalling pathways. *Nature* 376:188-191.
31. McConnell, J. E., J. F. Armstrong, P. E. Hodges, and J. B. Bard. 1995. The mouse 14-3-3 epsilon isoform, a kinase regulator whose expression pattern is modulated in mesenchyme and neuronal differentiation. *Dev Biol* 169:218-228.
32. Perego, L., and G. Berruti. 1997. Molecular cloning and tissue-specific expression of the mouse homologue of the rat brain 14-3-3 theta protein: characterization of its cellular and developmental pattern of expression in the male germ line. *Mol Reprod Dev* 47:370-379.
33. Umahara, T., T. Uchihara, K. Tsuchiya, A. Nakamura, T. Iwamoto, K. Ikeda, and M. Takasaki. 2004. 14-3-3 proteins and zeta isoform

containing neurofibrillary tangles in patients with Alzheimer's disease.
Acta Neuropathol 108:279-286.

34. Megidish, T., J. Cooper, L. Zhang, H. Fu, and S. Hakomori. 1998. A novel sphingosine-dependent protein kinase (SDK1) specifically phosphorylates certain isoforms of 14-3-3 protein. *J Biol Chem* 273:21834-21845.
35. Aitken, A., S. Howell, D. Jones, J. Madrazo, and Y. Patel. 1995. 14-3-3 alpha and delta are the phosphorylated forms of raf-activating 14-3-3 beta and zeta. In vivo stoichiometric phosphorylation in brain at a Ser-Pro-Glu-Lys MOTIF. *J Biol Chem* 270:5706-5709.
36. Dubois, T., C. Rommel, S. Howell, U. Steinhussen, Y. Soneji, N. Morrice, K. Moelling, and A. Aitken. 1997. 14-3-3 is phosphorylated by casein kinase I on residue 233. Phosphorylation at this site in vivo regulates Raf/14-3-3 interaction. *J Biol Chem* 272:28882-28888.
37. Tzivion, G., Y. H. Shen, and J. Zhu. 2001. 14-3-3 proteins; bringing new definitions to scaffolding. *Oncogene* 20:6331-6338.
38. Tzivion, G., Z. J. Luo, and J. Avruch. 2000. Calyculin A-induced vimentin phosphorylation sequesters 14-3-3 and displaces other 14-3-3 partners in vivo. *J Biol Chem* 275:29772-29778.
39. Shen, Y. H., J. Godlewski, A. Bronisz, J. Zhu, M. J. Comb, J. Avruch, and G. Tzivion. 2003. Significance of 14-3-3 self-dimerization for phosphorylation-dependent target binding. *Mol Biol Cell* 14:4721-4733.

40. Chan, T. A., H. Hermeking, C. Lengauer, K. W. Kinzler, and B. Vogelstein. 1999. 14-3-3Sigma is required to prevent mitotic catastrophe after DNA damage. *Nature* 401:616-620.
41. Yang, H. Y., Y. Y. Wen, C. H. Chen, G. Lozano, and M. H. Lee. 2003. 14-3-3 sigma positively regulates p53 and suppresses tumor growth. *Mol Cell Biol* 23:7096-7107.
42. Hermeking, H., C. Lengauer, K. Polyak, T. C. He, L. Zhang, S. Thiagalingam, K. W. Kinzler, and B. Vogelstein. 1997. 14-3-3 sigma is a p53-regulated inhibitor of G2/M progression. *Mol Cell* 1:3-11.
43. Jeanteur, P. 2000. [14-3-3sigma (stratifin), a potential tumor suppressor frequently inactivated by methylation in cancer of the breast]. *Bull Cancer* 87:525.
44. Suzuki, H., F. Itoh, M. Toyota, T. Kikuchi, H. Kakiuchi, and K. Imai. 2000. Inactivation of the 14-3-3 sigma gene is associated with 5' CpG island hypermethylation in human cancers. *Cancer Res* 60:4353-4357.
45. Iwata, N., H. Yamamoto, S. Sasaki, F. Itoh, H. Suzuki, T. Kikuchi, H. Kaneto, S. Iku, I. Ozeki, Y. Karino, T. Satoh, J. Toyota, M. Satoh, T. Endo, and K. Imai. 2000. Frequent hypermethylation of CpG islands and loss of expression of the 14-3-3 sigma gene in human hepatocellular carcinoma. *Oncogene* 19:5298-5302.

46. Ferguson, A. T., E. Evron, C. B. Umbricht, T. K. Pandita, T. A. Chan, H. Hermeking, J. R. Marks, A. R. Lambers, P. A. Futreal, M. R. Stampfer, and S. Sukumar. 2000. High frequency of hypermethylation at the 14-3-3 sigma locus leads to gene silencing in breast cancer. *Proc Natl Acad Sci U S A* 97:6049-6054.
47. Ling, C., D. Zuo, B. Xue, S. Muthuswamy, and W. J. Muller. A novel role for 14-3-3sigma in regulating epithelial cell polarity. *Genes Dev* 24:947-956.
48. McGonigle, S., M. J. Beall, E. L. Feeney, and E. J. Pearce. 2001. Conserved role for 14-3-3epsilon downstream of type I TGFbeta receptors. *FEBS Lett* 490:65-69.
49. Kim, H., J. H. Lee, and Y. Lee. 2003. Regulation of poly(A) polymerase by 14-3-3epsilon. *EMBO J* 22:5208-5219.
50. Toyo-oka, K., A. Shionoya, M. J. Gambello, C. Cardoso, R. Leventer, H. L. Ward, R. Ayala, L. H. Tsai, W. Dobyns, D. Ledbetter, S. Hirotsume, and A. Wynshaw-Boris. 2003. 14-3-3epsilon is important for neuronal migration by binding to NUDEL: a molecular explanation for Miller-Dieker syndrome. *Nat Genet* 34:274-285.
51. Autieri, M. V., and C. J. Carbone. 1999. 14-3-3Gamma interacts with and is phosphorylated by multiple protein kinase C isoforms in PDGF-

- stimulated human vascular smooth muscle cells. *DNA Cell Biol* 18:555-564.
52. Steinacker, P., P. Schwarz, K. Reim, P. Brechlin, O. Jahn, H. Kratzin, A. Aitken, J. Wiltfang, A. Aguzzi, E. Bahn, H. C. Baxter, N. Brose, and M. Otto. 2005. Unchanged survival rates of 14-3-3gamma knockout mice after inoculation with pathological prion protein. *Mol Cell Biol* 25:1339-1346.
 53. Wang, B., S. Ling, and W. C. Lin. 14-3-3Tau regulates Beclin 1 and is required for autophagy. *PLoS One* 5:e10409.
 54. Lau, J. M., X. Jin, J. Ren, J. Avery, B. J. DeBosch, I. Treskov, T. S. Lupu, A. Kovacs, C. Weinheimer, and A. J. Muslin. 2007. The 14-3-3tau phosphoserine-binding protein is required for cardiomyocyte survival. *Mol Cell Biol* 27:1455-1466.
 55. Richard, M., A. G. Biacabe, N. Streichenberger, J. W. Ironside, M. Mohr, N. Kopp, and A. Perret-Liaudet. 2003. Immunohistochemical localization of 14.3.3 zeta protein in amyloid plaques in human spongiform encephalopathies. *Acta Neuropathol* 105:296-302.
 56. Mateo, I., J. Llorca, J. Infante, E. Rodriguez-Rodriguez, J. Berciano, and O. Combarros. 2008. Gene-gene interaction between 14-3-3 zeta and butyrylcholinesterase modulates Alzheimer's disease risk. *Eur J Neurol* 15:219-222.

57. Lamba, S., V. Ravichandran, and E. O. Major. 2009. Glial cell type-specific subcellular localization of 14-3-3 zeta: an implication for JCV tropism. *Glia* 57:971-977.
58. Hernandez-Ruiz, L., F. Valverde, M. D. Jimenez-Nunez, E. Ocana, A. Saez-Benito, J. Rodriguez-Martorell, J. C. Bohorquez, A. Serrano, and F. A. Ruiz. 2007. Organellar proteomics of human platelet dense granules reveals that 14-3-3zeta is a granule protein related to atherosclerosis. *J Proteome Res* 6:4449-4457.
59. Omi, K., N. S. Hachiya, M. Tanaka, K. Tokunaga, and K. Kaneko. 2008. 14-3-3zeta is indispensable for aggregate formation of polyglutamine-expanded huntingtin protein. *Neurosci Lett* 431:45-50.
60. Fan, T., R. Li, N. W. Todd, Q. Qiu, H. B. Fang, H. Wang, J. Shen, R. Y. Zhao, N. P. Caraway, R. L. Katz, S. A. Stass, and F. Jiang. 2007. Up-regulation of 14-3-3zeta in lung cancer and its implication as prognostic and therapeutic target. *Cancer Res* 67:7901-7906.
61. Li, Z., J. Zhao, Y. Du, H. R. Park, S. Y. Sun, L. Bernal-Mizrachi, A. Aitken, F. R. Khuri, and H. Fu. 2008. Down-regulation of 14-3-3zeta suppresses anchorage-independent growth of lung cancer cells through anoikis activation. *Proc Natl Acad Sci U S A* 105:162-167.
62. Neal, C. L., J. Yao, W. Yang, X. Zhou, N. T. Nguyen, J. Lu, C. G. Danes, H. Guo, K. H. Lan, J. Ensor, W. Hittelman, M. C. Hung, and D. Yu. 2009.

- 14-3-3zeta overexpression defines high risk for breast cancer recurrence and promotes cancer cell survival. *Cancer Res* 69:3425-3432.
63. Lu, J., H. Guo, W. Treekitkarnmongkol, P. Li, J. Zhang, B. Shi, C. Ling, X. Zhou, T. Chen, P. J. Chiao, X. Feng, V. L. Seewaldt, W. J. Muller, A. Sahin, M. C. Hung, and D. Yu. 2009. 14-3-3zeta Cooperates with ErbB2 to promote ductal carcinoma in situ progression to invasive breast cancer by inducing epithelial-mesenchymal transition. *Cancer Cell* 16:195-207.
 64. Kobayashi, R., M. Deavers, R. Patenia, T. Rice-Stitt, J. Halbe, S. Gallardo, and R. S. Freedman. 2009. 14-3-3 zeta protein secreted by tumor associated monocytes/macrophages from ascites of epithelial ovarian cancer patients. *Cancer Immunol Immunother* 58:247-258.
 65. Lin, M., C. D. Morrison, S. Jones, N. Mohamed, J. Bacher, and C. Plass. 2009. Copy number gain and oncogenic activity of YWHAZ/14-3-3zeta in head and neck squamous cell carcinoma. *Int J Cancer* 125:603-611.
 66. Matta, A., S. Bahadur, R. Duggal, S. D. Gupta, and R. Ralhan. 2007. Over-expression of 14-3-3zeta is an early event in oral cancer. *BMC Cancer* 7:169.
 67. Maxwell, S. A., Z. Li, D. Jaye, S. Ballard, J. Ferrell, and H. Fu. 2009. 14-3-3zeta mediates resistance of diffuse large B cell lymphoma to an anthracycline-based chemotherapeutic regimen. *J Biol Chem* 284:22379-22389.

68. Li, Y., L. Zou, Q. Li, B. Haibe-Kains, R. Tian, C. Desmedt, C. Sotiriou, Z. Szallasi, J. D. Iglehart, A. L. Richardson, and Z. C. Wang. Amplification of LAPTM4B and YWHAZ contributes to chemotherapy resistance and recurrence of breast cancer. *Nat Med* 16:214-218.
69. Danes, C. G., S. L. Wyszomierski, J. Lu, C. L. Neal, W. Yang, and D. Yu. 2008. 14-3-3 zeta down-regulates p53 in mammary epithelial cells and confers luminal filling. *Cancer Res* 68:1760-1767.
70. Neal, C. L., and D. Yu. 14-3-3zeta as a prognostic marker and therapeutic target for cancer. *Expert Opin Ther Targets* 14:1343-1354.
71. Bartel, D. P. 2004. MicroRNAs: genomics, biogenesis, mechanism, and function. *Cell* 116:281-297.
72. van Rooij, E., W. S. Marshall, and E. N. Olson. 2008. Toward microRNA-based therapeutics for heart disease: the sense in antisense. *Circ Res* 103:919-928.
73. He, L., and G. J. Hannon. 2004. MicroRNAs: small RNAs with a big role in gene regulation. *Nat Rev Genet* 5:522-531.
74. Lewis, B. P., C. B. Burge, and D. P. Bartel. 2005. Conserved seed pairing, often flanked by adenosines, indicates that thousands of human genes are microRNA targets. *Cell* 120:15-20.

75. Ambros, V. 2004. The functions of animal microRNAs. *Nature* 431:350-355.
76. Wang, S., A. B. Aurora, B. A. Johnson, X. Qi, J. McAnally, J. A. Hill, J. A. Richardson, R. Bassel-Duby, and E. N. Olson. 2008. The endothelial-specific microRNA miR-126 governs vascular integrity and angiogenesis. *Dev Cell* 15:261-271.
77. Fish, J. E., M. M. Santoro, S. U. Morton, S. Yu, R. F. Yeh, J. D. Wythe, K. N. Ivey, B. G. Bruneau, D. Y. Stainier, and D. Srivastava. 2008. miR-126 regulates angiogenic signaling and vascular integrity. *Dev Cell* 15:272-284.
78. Nicoli, S., C. Standley, P. Walker, A. Hurlstone, K. E. Fogarty, and N. D. Lawson. MicroRNA-mediated integration of haemodynamics and Vegf signalling during angiogenesis. *Nature* 464:1196-1200.
79. Zampetaki, A., S. Kiechl, I. Drozdov, P. Willeit, U. Mayr, M. Prokopi, A. Mayr, S. Weger, F. Oberhollenzer, E. Bonora, A. Shah, J. Willeit, and M. Mayr. Plasma microRNA profiling reveals loss of endothelial miR-126 and other microRNAs in type 2 diabetes. *Circ Res* 107:810-817.
80. El-Assaad, F., C. Hempel, V. Combes, A. J. Mitchell, H. J. Ball, J. A. Kurtzhals, N. H. Hunt, J. M. Mathys, and G. E. Grau. Differential microRNA expression in experimental cerebral and noncerebral malaria. *Infect Immun* 79:2379-2384.

81. Fichtlscherer, S., S. De Rosa, H. Fox, T. Schwietz, A. Fischer, C. Liebetrau, M. Weber, C. W. Hamm, T. Roxel, M. Muller-Ardogan, A. Bonauer, A. M. Zeiher, and S. Dimmeler. Circulating microRNAs in patients with coronary artery disease. *Circ Res* 107:677-684.
82. Oglesby, I. K., I. M. Bray, S. H. Chotirmall, R. L. Stallings, S. J. O'Neill, N. G. McElvaney, and C. M. Greene. miR-126 is downregulated in cystic fibrosis airway epithelial cells and regulates TOM1 expression. *J Immunol* 184:1702-1709.
83. Otsubo, T., Y. Akiyama, Y. Hashimoto, S. Shimada, K. Goto, and Y. Yuasa. MicroRNA-126 inhibits SOX2 expression and contributes to gastric carcinogenesis. *PLoS One* 6:e16617.
84. Negrini, M., and G. A. Calin. 2008. Breast cancer metastasis: a microRNA story. *Breast Cancer Res* 10:203.
85. Wang, X., S. Tang, S. Y. Le, R. Lu, J. S. Rader, C. Meyers, and Z. M. Zheng. 2008. Aberrant expression of oncogenic and tumor-suppressive microRNAs in cervical cancer is required for cancer cell growth. *PLoS One* 3:e2557.
86. Ciafre, S. A., S. Galardi, A. Mangiola, M. Ferracin, C. G. Liu, G. Sabatino, M. Negrini, G. Maira, C. M. Croce, and M. G. Farace. 2005. Extensive modulation of a set of microRNAs in primary glioblastoma. *Biochem Biophys Res Commun* 334:1351-1358.

87. Meister, J., and M. H. Schmidt. miR-126 and miR-126*: new players in cancer. *ScientificWorldJournal* 10:2090-2100.
88. Neal, C. L., J. Xu, P. Li, S. Mori, J. Yang, N. N. Neal, X. Zhou, S. L. Wyszomierski, and D. Yu. Overexpression of 14-3-3zeta in cancer cells activates PI3K via binding the p85 regulatory subunit. *Oncogene*.
89. Seimiya, H., H. Sawada, Y. Muramatsu, M. Shimizu, K. Ohko, K. Yamane, and T. Tsuruo. 2000. Involvement of 14-3-3 proteins in nuclear localization of telomerase. *EMBO J* 19:2652-2661.
90. Turgeon, B., and S. Meloche. 2009. Interpreting neonatal lethal phenotypes in mouse mutants: insights into gene function and human diseases. *Physiol Rev* 89:1-26.
91. Harris, T. A., M. Yamakuchi, M. Ferlito, J. T. Mendell, and C. J. Lowenstein. 2008. MicroRNA-126 regulates endothelial expression of vascular cell adhesion molecule 1. *Proc Natl Acad Sci U S A* 105:1516-1521.
92. Cullere, X., P. Rose, U. Thathamangalam, A. Chatterjee, K. P. Mullane, D. C. Pallas, T. L. Benjamin, T. M. Roberts, and B. S. Schaffhausen. 1998. Serine 257 phosphorylation regulates association of polyomavirus middle T antigen with 14-3-3 proteins. *J Virol* 72:558-563.

93. Tavazoie, S. F., C. Alarcon, T. Oskarsson, D. Padua, Q. Wang, P. D. Bos, W. L. Gerald, and J. Massague. 2008. Endogenous human microRNAs that suppress breast cancer metastasis. *Nature* 451:147-152.
94. Zhu, N., D. Zhang, H. Xie, Z. Zhou, H. Chen, T. Hu, Y. Bai, Y. Shen, W. Yuan, Q. Jing, and Y. Qin. Endothelial-specific intron-derived miR-126 is down-regulated in human breast cancer and targets both VEGFA and PIK3R2. *Mol Cell Biochem* 351:157-164.
95. Hasegawa, Y., K. Fujii, M. Yamada, Y. Igarashi, K. Tachibana, T. Tanaka, K. Onigata, Y. Nishi, S. Kato, and T. Hasegawa. 2000. Identification of novel human GH-1 gene polymorphisms that are associated with growth hormone secretion and height. *J Clin Endocrinol Metab* 85:1290-1295.
96. Hiney, J. K., V. Srivastava, C. L. Nyberg, S. R. Ojeda, and W. L. Dees. 1996. Insulin-like growth factor I of peripheral origin acts centrally to accelerate the initiation of female puberty. *Endocrinology* 137:3717-3728.
97. Copeland, K. C., T. J. Kuehl, and V. D. Castracane. 1982. Pubertal endocrinology of the baboon: elevated somatomedin-C/insulin-like growth factor I at puberty. *J Clin Endocrinol Metab* 55:1198-1201.
98. Xu, J., L. Liao, G. Ning, H. Yoshida-Komiya, C. Deng, and B. W. O'Malley. 2000. The steroid receptor coactivator SRC-3 (p/CIP/RAC3/AIB1/ACTR/TRAM-1) is required for normal growth, puberty,

female reproductive function, and mammary gland development. *Proc Natl Acad Sci U S A* 97:6379-6384.

99. Saltiel, A. R., and C. R. Kahn. 2001. Insulin signalling and the regulation of glucose and lipid metabolism. *Nature* 414:799-806.
100. Yakar, S., J. L. Liu, A. M. Fernandez, Y. Wu, A. V. Schally, J. Frystyk, S. D. Chernausek, W. Mejia, and D. Le Roith. 2001. Liver-specific igf-1 gene deletion leads to muscle insulin insensitivity. *Diabetes* 50:1110-1118.
101. Wang, H. Q., D. A. Altomare, K. L. Skele, P. I. Poulikakos, F. P. Kuhajda, A. Di Cristofano, and J. R. Testa. 2005. Positive feedback regulation between AKT activation and fatty acid synthase expression in ovarian carcinoma cells. *Oncogene* 24:3574-3582.
102. Semenza, G. L., P. H. Roth, H. M. Fang, and G. L. Wang. 1994. Transcriptional regulation of genes encoding glycolytic enzymes by hypoxia-inducible factor 1. *J Biol Chem* 269:23757-23763.
103. Ryan, H. E., J. Lo, and R. S. Johnson. 1998. HIF-1 alpha is required for solid tumor formation and embryonic vascularization. *EMBO J* 17:3005-3015.
104. Denko, N. C. 2008. Hypoxia, HIF1 and glucose metabolism in the solid tumour. *Nat Rev Cancer*.

105. Withers, D. J., D. J. Burks, H. H. Towery, S. L. Altamuro, C. L. Flint, and M. F. White. 1999. Irs-2 coordinates Igf-1 receptor-mediated beta-cell development and peripheral insulin signalling. *Nat Genet* 23:32-40.
106. Liu, J. P., J. Baker, A. S. Perkins, E. J. Robertson, and A. Efstratiadis. 1993. Mice carrying null mutations of the genes encoding insulin-like growth factor I (Igf-1) and type 1 IGF receptor (Igf1r). *Cell* 75:59-72.
107. Kleinberg, D. L., M. Feldman, and W. Ruan. 2000. IGF-I: an essential factor in terminal end bud formation and ductal morphogenesis. *J Mammary Gland Biol Neoplasia* 5:7-17.
108. Shang, Y., Y. Mao, J. Batson, S. J. Scales, G. Phillips, M. R. Lackner, K. Totpal, S. Williams, J. Yang, Z. Tang, Z. Modrusan, C. Tan, W. C. Liang, S. P. Tsai, A. Vanderbilt, K. Kozuka, K. Hoefflich, J. Tien, S. Ross, C. Li, S. H. Lee, A. Song, Y. Wu, J. P. Stephan, A. Ashkenazi, and J. Zha. 2008. Antixenograft tumor activity of a humanized anti-insulin-like growth factor-I receptor monoclonal antibody is associated with decreased AKT activation and glucose uptake. *Mol Cancer Ther* 7:2599-2608.
109. Graham, M. R., P. Evans, N. E. Thomas, B. Davies, and J. S. Baker. 2009. Changes in endothelial dysfunction and associated cardiovascular disease morbidity markers in GH-IGF axis pathology. *Am J Cardiovasc Drugs* 9:371-381.

110. Abuzzahab, M. J., A. Schneider, A. Goddard, F. Grigorescu, C. Lautier, E. Keller, W. Kiess, J. Klammt, J. Kratzsch, D. Osgood, R. Pfaffle, K. Raile, B. Seidel, R. J. Smith, and S. D. Chernausek. 2003. IGF-I receptor mutations resulting in intrauterine and postnatal growth retardation. *N Engl J Med* 349:2211-2222.
111. Raile, K., J. Klammt, A. Schneider, A. Keller, S. Laue, R. Smith, R. Pfaffle, J. Kratzsch, E. Keller, and W. Kiess. 2006. Clinical and functional characteristics of the human Arg59Ter insulin-like growth factor i receptor (IGF1R) mutation: implications for a gene dosage effect of the human IGF1R. *J Clin Endocrinol Metab* 91:2264-2271.
112. Kawashima, Y., S. Kanzaki, F. Yang, T. Kinoshita, K. Hanaki, J. Nagaishi, Y. Ohtsuka, I. Hisatome, H. Ninomoya, E. Nanba, T. Fukushima, and S. Takahashi. 2005. Mutation at cleavage site of insulin-like growth factor receptor in a short-stature child born with intrauterine growth retardation. *J Clin Endocrinol Metab* 90:4679-4687.
113. Inagaki, K., A. Tiulpakov, P. Rubtsov, P. Sverdlova, V. Peterkova, S. Yakar, S. Terekhov, and D. LeRoith. 2007. A familial insulin-like growth factor-I receptor mutant leads to short stature: clinical and biochemical characterization. *J Clin Endocrinol Metab* 92:1542-1548.
114. Kulkarni, R. N., M. Holzenberger, D. Q. Shih, U. Ozcan, M. Stoffel, M. A. Magnuson, and C. R. Kahn. 2002. beta-cell-specific deletion of the Igf1

receptor leads to hyperinsulinemia and glucose intolerance but does not alter beta-cell mass. *Nat Genet* 31:111-115.

115. Fernandez, A. M., J. K. Kim, S. Yakar, J. Dupont, C. Hernandez-Sanchez, A. L. Castle, J. Filmore, G. I. Shulman, and D. Le Roith. 2001. Functional inactivation of the IGF-I and insulin receptors in skeletal muscle causes type 2 diabetes. *Genes Dev* 15:1926-1934.
116. Arteaga, C. L. 1992. Interference of the IGF system as a strategy to inhibit breast cancer growth. *Breast Cancer Res Treat* 22:101-106.
117. Mohanraj, L., and Y. Oh. Targeting IGF-I, IGFBPs and IGF-I receptor system in cancer: the current and future in breast cancer therapy. *Recent Pat Anticancer Drug Discov* 6:166-177.
118. Dang, C. V., M. Hamaker, P. Sun, A. Le, and P. Gao. Therapeutic targeting of cancer cell metabolism. *J Mol Med (Berl)* 89:205-212.
119. Kim, J. W., P. Gao, and C. V. Dang. 2007. Effects of hypoxia on tumor metabolism. *Cancer Metastasis Rev* 26:291-298.
120. Kroemer, G., and J. Pouyssegur. 2008. Tumor cell metabolism: cancer's Achilles' heel. *Cancer Cell* 13:472-482.
121. Ravi, R., B. Mookerjee, Z. M. Bhujwalla, C. H. Sutter, D. Artemov, Q. Zeng, L. E. Dillehay, A. Madan, G. L. Semenza, and A. Bedi. 2000.

Regulation of tumor angiogenesis by p53-induced degradation of hypoxia-inducible factor 1alpha. *Genes Dev* 14:34-44.

122. Pollard, P. J., J. J. Briere, N. A. Alam, J. Barwell, E. Barclay, N. C. Wortham, T. Hunt, M. Mitchell, S. Olpin, S. J. Moat, I. P. Hargreaves, S. J. Heales, Y. L. Chung, J. R. Griffiths, A. Dalgleish, J. A. McGrath, M. J. Gleeson, S. V. Hodgson, R. Poulson, P. Rustin, and I. P. Tomlinson. 2005. Accumulation of Krebs cycle intermediates and over-expression of HIF1alpha in tumours which result from germline FH and SDH mutations. *Hum Mol Genet* 14:2231-2239.
123. Sano, M., T. Minamino, H. Toko, H. Miyauchi, M. Orimo, Y. Qin, H. Akazawa, K. Tateno, Y. Kayama, M. Harada, I. Shimizu, T. Asahara, H. Hamada, S. Tomita, J. D. Molkentin, Y. Zou, and I. Komuro. 2007. p53-induced inhibition of Hif-1 causes cardiac dysfunction during pressure overload. *Nature* 446:444-448.
124. Kondo, T., D. Vicent, K. Suzuma, M. Yanagisawa, G. L. King, M. Holzenberger, and C. R. Kahn. 2003. Knockout of insulin and IGF-1 receptors on vascular endothelial cells protects against retinal neovascularization. *J Clin Invest* 111:1835-1842.
125. Lambooi, A. C., K. H. van Wely, D. J. Lindenbergh-Kortleve, R. W. Kuijpers, M. Kliffen, and C. M. Mooy. 2003. Insulin-like growth factor-I and its receptor in neovascular age-related macular degeneration. *Invest Ophthalmol Vis Sci* 44:2192-2198.

126. Bernardi, R., I. Guernah, D. Jin, S. Grisendi, A. Alimonti, J. Teruya-Feldstein, C. Cordon-Cardo, M. C. Simon, S. Rafii, and P. P. Pandolfi. 2006. PML inhibits HIF-1alpha translation and neoangiogenesis through repression of mTOR. *Nature* 442:779-785.
127. Yuan, T., Y. Wang, Z. J. Zhao, and H. Gu. Protein-tyrosine phosphatase PTPN9 negatively regulates ErbB2 and epidermal growth factor receptor signaling in breast cancer cells. *J Biol Chem* 285:14861-14870.
128. Huang, X., E. Gschwend, B. Van Handel, D. Cheng, H. K. Mikkola, and O. N. Witte. Regulated expression of microRNAs-126/126* inhibits erythropoiesis from human embryonic stem cells. *Blood* 117:2157-2165.
129. Cho, C. Y., S. H. Koo, Y. Wang, S. Callaway, S. Hedrick, P. A. Mak, A. P. Orth, E. C. Peters, E. Saez, M. Montminy, P. G. Schultz, and S. K. Chanda. 2006. Identification of the tyrosine phosphatase PTP-MEG2 as an antagonist of hepatic insulin signaling. *Cell Metab* 3:367-378.
130. Chen, M., J. P. Sun, J. Liu, and X. Yu. [Research progress of several protein tyrosine phosphatases in diabetes]. *Sheng Li Xue Bao* 62:179-189.

VITA

Jun Yang was born November 8th, 1978 in Shanghai China. He graduated from Fudan University in China in 2001 having his thesis work done in Dr. Li Jin's laboratory. Then he worked as a research assistant in Shanghai Institute of Biochemistry and Cell Biology, Chinese Academy of Sciences with Dr. Yonglian Zhang for two years. On 2003, he enrolled in the University of Texas Health Science Center at Houston Graduate School of Biomedical Sciences. He had his graduate training in Dr. Dihua Yu's lab.

Permanent address

2703 Catalina Shores Dr.

Pearland, TX 77584